Supplement of Atmos. Meas. Tech., 19, 7585–7605, 2026
https://doi.org/10.5194/amt-19-7585-2026-supplement
© Author(s) 2026. CC BY 4.0 License.



Atmospheric Measurement Techniques
Open Access
EGU

*Supplement of*

# Single-blind controlled release testing of vehicle- and aircraft-based methane measurement systems at the TADI facility

**Audrey McManemin et al.**

*Correspondence to:* Audrey McManemin (anm49@stanford.edu)

The copyright of individual parts of the supplement might differ from the article licence.

**Table of Contents**

*List of Figures* ..... *5*

*List of Tables* ..... *7*

*S1 Experimental Setup* ..... *9*

**S1.1 TADI Test Site Description** ..... **9**

S1.1.1 TADI Team ..... 11

**S1.2 Methane Release Schedule and Emission Rates** ..... **11**

S1.2.1 Zero Releases ..... 12

S1.2.2 Satellite Releases ..... 13

S1.2.3 Methane release flowrates and schedules ..... 13

**S1.3 Participant Scheduling** ..... **20**

S1.3.1 FAAM Scheduling ..... 21

*S2 Participant & Technology Descriptions* ..... *21*

**S2.1 Description of Academic Institutions and Deployed Technology** ..... **23**

S2.1.1 Technical University of Denmark (DTU) ..... 23

S2.1.2 Heidelberg University (UHEI) ..... 24

S2.1.3 The Cyprus Institute (CYI), Royal Holloway University of London (RHUL), Utrecht University (UU), and the Laboratory for Climate and Environmental Sciences (France) (LSCE) ..... 25

S2.1.4 Swiss Federal Laboratories for Materials Science and Technology and University of Zurich (Empa/UZH) ..... 25

S2.1.5 FAAM Airborne Laboratory ..... 27

**S2.2 Flight Operator Descriptions** ..... **33**

S2.2.1 Swiss Flight Services ..... 33

**S2.3 Participant Technology Survey Responses** ..... **33**

S2.3.1 DTU Technology Survey Responses ..... 34

S2.3.2 UHEI Technology Survey Responses ..... 35

S2.3.3 UU/LSCE/CYI/RHUL Technology Survey Responses ..... 36

S2.3.4 Empa/UZH Technology Survey Responses ..... 37
S2.3.5 FAAM Technology Survey Responses ..... 40
*S3 Field Data Collection* ..... *42*
**S3.1 Field Data Collection Procedures** ..... **42**
**S3.2 Weather Conditions** ..... **42**
**S3.3 Wind Rose Plots** ..... **45**
*S4 Participant Data Collection, Reporting, and Filtering* ..... *50*
**S4.1 Participant Submission & Data Cleaning** ..... **51**
S4.1.1 Data filtering and categorization methods ..... 51
S4.1.2 DTU Data Cleaning ..... 52
S4.1.3 UHEI Data Cleaning ..... 53
S4.1.4 UU/LSCE/CYI/RHUL Data Cleaning ..... 54
S4.1.5 Empa/UZH Data Cleaning ..... 55
S4.1.6 FAAM Data Cleaning ..... 56
**S4.2 Data classification** ..... **57**
**S4.3 Solution Uncertainties** ..... **58**
*S5 Detection Results* ..... *59*
**S5.1 Release Classification Criteria** ..... **59**
**S5.2 Detection Capabilities Under 5 kg/h** ..... **59**
**S5.3 Distribution of Detected Releases** ..... **60**
**S5.4 UHEI non-zero release detection** ..... **60**
*S6 Quantification Results* ..... *61*
**S6.1 Parity Plots for Releases Below 100 kg $h^{-1}$ and Above 10 kg $h^{-1}$** ..... **61**
**S6.2 Participant Parity Plots** ..... **62**
**S6.3 Uncertainty-weighted Regression of Quantification Estimates** ..... **64**
*S7 Wind Condition Analysis* ..... *66*
***References*** ..... *Error! Bookmark not defined.*

**List of Figures**

Figure S1. Map of the TADI test site. ..... 10

Figure S2. Side view of TADI gas release platform. ..... 11

Figure S3. Performance in-flight "target" measurements for six missions flown in 2024 (two in June, two in September, two in October) to determine 10 Hz $CH_4$ measurements bias and precision. The dashed box indicates the data obtained during the TADI controlled release experiment on 12 September. ..... 28

**Figure S4.** Flight-track of the FAAM aircraft during mission C388 (12 September 2024). The 2 NM radius red circle is centered around the TADI facility. ..... 30

Figure S5. Example of $CH_4$ plume (10 Hz resolution) detected between 14:31:18.8 and 14:31:32.0 UTC at 191 m above ground level ..... 31

Figure S6. Heat maps of CH4, SO2, NO2 and CO2 mole fractions of during an anticlockwise orbit around TADI site ..... 31

Figure S7. Timeseries of $CH_4$, $SO_2$, $NO_2$ and $CO_2$ mole fractions of during an anticlockwise orbit around TADI site ..... 32

Figure S8. Wind rose plots characterizing the wind conditions during specific releases in Week 1 and 4. ..... 45

Figure S9. Week 1 wind rose plots by release. ..... 46

Figure S10. Week 2 wind rose plots by release. ..... 47

Figure S11. Week 3 wind rose plots by release ..... 48

Figure S12. Week 4 wind rose plots by release. ..... 49

Figure S13. Stanford QC process release estimate classification criteria. ..... 52

Figure S14. Data cleaning process flowchart for DTU ..... 53

Figure S15. Data cleaning process flowchart for UHEI. ..... 54

Figure S16. Data cleaning process flowchart for UU/LSCE/CYI/RHUL. ..... 55

Figure S17. Data cleaning process flowchart for Empa/UZH. ..... 56

Figure S18. Data cleaning process flowchart for FAAM. ..... 57

Figure S19. Detection capabilities below 5 kg $h^{-1}$. ..... 59

Figure S20. Distribution of detected releases by participant. ..... 60

Figure S21. Parity plots with true release rates of <100 kg $h^{-1}$ ..... 61
Figure S22. Parity plots with true release rates > 10 kg $h^{-1}$ ..... 62
Figure S23. DTU parity plot. ..... 63
Figure S24. UHEI parity plot. ..... 63
Figure S25. UU/LSCE/CYI/RHUL parity plot. ..... 63
Figure S26. Empa/UZH parity plot. ..... 64
Figure S27. FAAM parity plot. ..... 64
Figure S28. Parity plots for the academic teams showing the unweighted (OLS, solid black) and uncertainty-weighted (WLS, dashed red) linear fits. ..... 65
Figure S29. Parity plots with average wind speeds. ..... 66
Figure S30. Parity plots with wind speed coefficient of variation (CoV). ..... 67
Figure S31. Parity plots with wind direction coefficient of variation (CoV). ..... 68
Figure S32. DTU quantification data by wind condition bin. ..... 70
Figure S33. UHEI quantification data by wind condition bin. ..... 71
Figure S34. UU/LSCE/CYI/RHUl quantification data by wind condition bin. ..... 72
Figure S35. Empa/UZH quantification data by wind condition bin. ..... 73
Figure S36. FAAM quantification data by wind condition bin. ..... 74

**List of Tables**

Table S1. Intended daily release schedule. ..... 11

Table S2. Daily, weekly, and campaign total number of releases. ..... 12

Table S3. Summary of zero releases and satellite-designated releases by week. ..... 13

Table S4. Week 1 methane release flowrates and times..... 13

Table S5. Week 2 methane release flowrates and times..... 15

Table S6. Week 3 methane release flowrates and times..... 17

Table S7. Week 4 methane release flowrates and times..... 18

Table S8. Schedule of participants and the week(s) that they participated in (including commercial teams). ..... 21

Table S9. Participant name, solution name, technology and sensor types, including commercial participants. ..... 21

Table S10. Previous controlled release testing of the participants..... 22

Table S11. Daily weather conditions. ..... 42

Table S12. Daily temperature conditions. ..... 43

Table S13. Daily wind conditions. ..... 44

Table S14. Results reporting dates and submission dates by participant and week. ..... 50

Table S15. Participant release estimate filtering criteria ..... 51

Table S16. DTU QC flags with number of releases and associated estimated emission rate. ..... 53

Table S17. UHEI QC flags with number of releases and associated estimated emission rate. .... 53

Table S18. UU/LSCE/CYI/RHUL QC flags with number of releases and associated estimated emission rate. ..... 54

Table S19. Empa/UZH QC flags with number of releases and associated estimated emission rate. ..... 55

Table S20. FAAM QC flags with number of releases and associated estimated emission rate.... 56

Table S21. Release counts by participant through the filtering process. ..... 57

Table S22. Maximum and minimum true release rates measured and passing the QC process. .. 58

Table S23. Uncertainty types associated with participant quantification of release flowrates. .... 58

Table S24. General release categorization criteria into TP, TN, FP, and FN. ..... 59

Table 25. Slope ($R^2$) values of the linear model fit on releases across technology types and wind analysis bins. Values are provided for bins that had more than one quantification estimate occurring under those wind conditions. FAAM and GHGSat only submitted one estimate, so a linear trend could not be fit to the data. ..... 69

Table S26. Number of data points in the bins of average wind speed, wind speed CoV, and wind direction CoV used in analysis. ..... 69

## S1 Experimental Setup

This section details the experimental setup, environmental monitoring, true release rates and release control operations, and other experimental methods. The results presented in this paper were collected at the same time as the results presented in McManemin et al. (2026), which contains the experimental results from the commercial teams participating in the controlled release testing. All experimental methods and data processing and analysis methods were the same for both sets of participants.

### S1.1 TADI Test Site Description

TADI (TotalEnergies Anomaly Detection Initiatives) is a research and development platform located in Lacq, France, specifically dedicated to testing and experimenting with gas leak detection and quantification technology (TotalEnergies, 2025a). Owned and operated by TotalEnergies, TADI was constructed to evaluate technologies aimed at improving safety and minimizing gas emissions on oil and gas production sites. TADI is located on an industrial SEVESO 3 site with active industrial activity around it. The leak points are located within dismantled oil and gas equipment, such as drum pipes, valves, wellheads, flanges, level gauges, etc. Originally designed for safety research in 2015, the site quickly evolved into being capable of testing greenhouse gas emission measurement technologies. The site can test gas detection and quantification capabilities of several types of gases, including methane. Since 2016, TADI and the Methane Emission Technology Evaluation Center (METEC) from Colorado State University have built a strong scientific collaboration. In 2023, TADI and METEC partnered to develop an international protocol for qualification of methane emissions technologies, which was updated in 2025 (Zimmerle et al., 2025; TotalEnergies, 2025b).

The TADI site is made up of the gas release platform and the surrounding area. The gas release platform is an ATEX zone and contains all the leak points. The gas release platform is 40m wide, and 50m in length, for area of 2000 $m^2$. There are two regions of the platform: TADI North and TADI South. TADI North can release methane flowrates of 0.0036 kg/h to 21.6 kg/h. TADI South can release flowrates from 0.54 kg/h to 1080 kg/h of methane. Other gases have different flowrate limitations due to safety and other constraints. The methane flow rate limit depends on the length of time the gas is released, as gas is supplied via CNG bottles. The equipment on TADI can provide 226 different leak scenarios, with different combinations of equipment, location on equipment, outlet diameter, and inlet diameter. There is a meteorological station permanently on TADI site, a 2d wind anemometer and a ZX 300 wind LIDAR. These data are not intended to be shared during testing, as performers must use their own equipment in the same configuration as during measurement campaigns.

Figure S1 contains a map of the test site. The releases are controlled from an operation room directly north of the platform. The control room was under the jurisdiction of the TADI site

engineer, and no participants were allowed in the control room to maintain the blind nature of the experiment. The Stanford team and any participants onsite were housed in a work room dedicated to the campaign set back from the platform. Due to its location on an active industrial site (INDUSLACQ), personal protective equipment (PPE), a gas mask, and a personal gas detector were required when anywhere on the industrial site except for the control room and campaign headquarters. Figure S2 depicts the gas release platform.

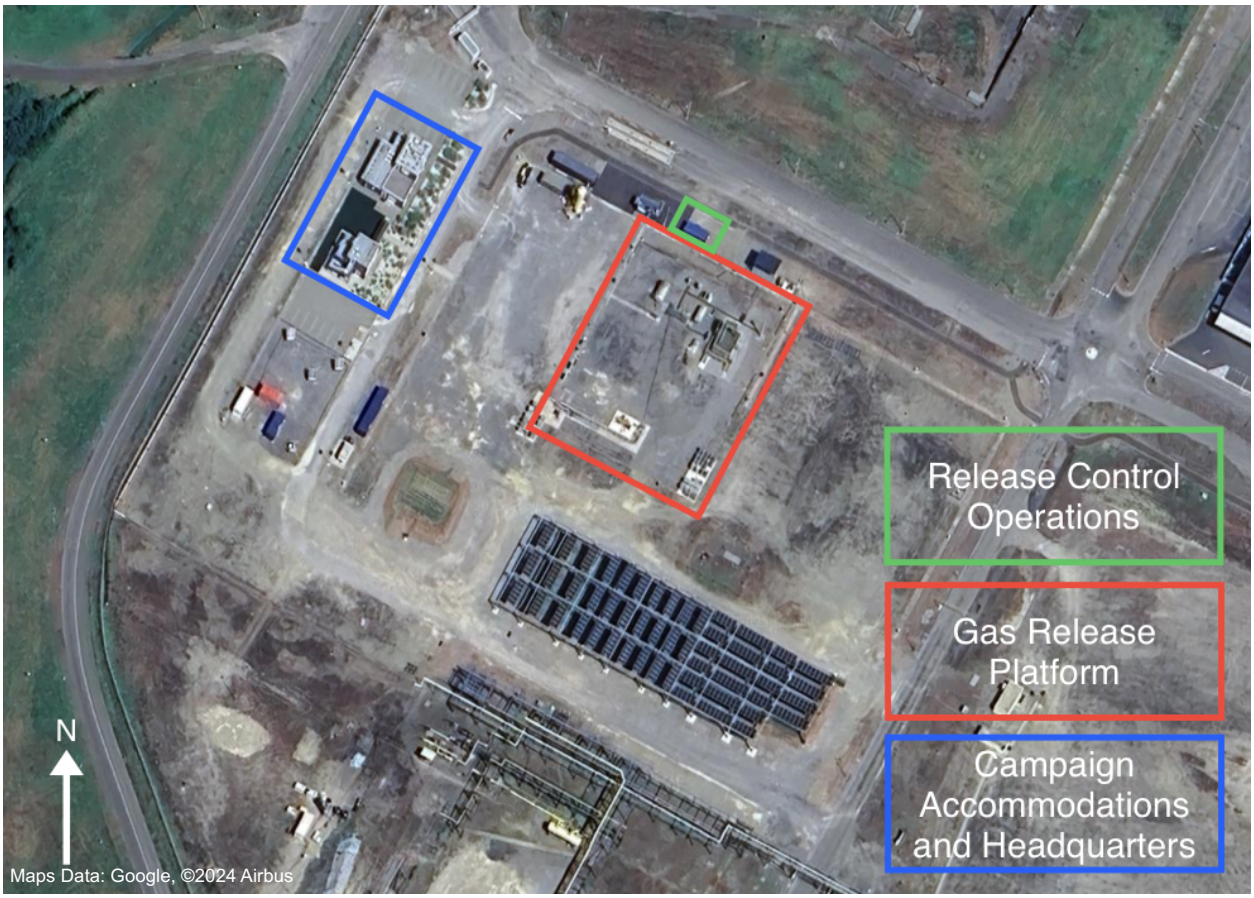



**Figure S1.** Map of the TADI test site.
The gas release platform is indicated in red, the gas release control room in green, and the campaign headquarters in blue.




**Figure S2.** Side view of TADI gas release platform.
The methane storage tanks are in the front of the picture, looking northeast. Note the control room (blue storage containers) in the upper left.

### S1.1.1 TADI Team

There was a team of dedicated engineers and researchers associated with TADI that helped plan and execute the experiment. Catherine Juéry, Vincent Blandin, Yvan Faucher, and Jordi Jourde were invaluable in ensuring a safe and seamless execution of the experiments.

## S1.2 Methane Release Schedule and Emission Rates

**Table S1.** Intended daily release schedule.

| Release Number | Start Time (Local) | End Time (Local) |
|---|---|---|
| 1 | 9:00 | 9:45 |
| 2 | 10:00 | 10:45 |
| 3 | 11:00 | 11:45 |
| 4 | 12:00 | 12:45 |
| 5 | 13:30 | 14:15 |
| 6 | 14:30 | 15:15 |

| | | |
|---|---|---|
| 7 | 15:30 | 16:15 |
| 8 | 16:30 | 17:15 |

Methane release flowrates ranged from 0 kg/h (so-called “zero release”) to 310 kg/h. The gas used in the experiment was sourced by the TADI team and was specified at ≥99% $CH_4$ composition. The release rates were different every week. Table S2 contains the daily and weekly total number of releases. The lower number of releases on Mondays (<8) was due to the safety briefing conducted Monday morning each week as participants arrived onsite for the first time.

**Table S2.** Daily, weekly, and campaign total number of releases.

| **Week** | **Number of Releases per Day** | | | | | **Weekly Total Number of Releases** |
|---|---|---|---|---|---|---|
| | *Monday* | *Tuesday* | *Wednesday* | *Thursday* | *Friday* | |
| Week 1 | 7 | 9 | 8 | 8 | 8 | 40 |
| Week 2 | 7 | 8 | 8 | 8 | 4 | 35 |
| Week 3 | 6 | 9 | 9 | 8 | 5 | 37 |
| Week 4 | 6 | 8 | 9 | 9 | 8 | 40 |
| *Campaign Total* | | | | | | 152 |

For a particular release, the TADI site participant would refer to the schedule and prepare the leak location during the break between releases. This would involve both physical operations (opening or closing valves, changing pipe configurations) and inputting the desired release characteristics in the control room (flowrate, location). The TADI site estimated a specific uncertainty between actual flowrate and the specified flowrate for methane for each release. The average uncertainty was 3.23%. There were two zero releases schedule for each week, and two to four satellite scale releases, depending on the week.

### S1.2.1 Zero Releases

There were two zero releases pre-scheduled for each week. These releases aim to test for false positive detections. Because false positives were not the primary focus of the testing campaign, only two release periods were designated as zero releases. Table S3 contains the

summary of actual number of zero releases conducted during each week, which can differ from the pre-scheduled two releases. Notably, Week 2 only had one zero release due to the Friday afternoon releases being canceled (see Sect. S5.4).

### S1.2.2 Satellite Releases

As discussed above, there were several releases each week that were specifically targeted to the commercial satellite participants and/or the FAAM aircraft. Due to the higher detection limit of satellites, these releases were designed to be high-volume releases. Other participants were not aware of the satellite schedule, nor which overpasses were selected by the Stanford and TADI teams and therefore did not know the timing of the high-volume releases.

During the June campaign, several of the satellite-designated releases occurred during cloud cover of the site, resulting in the satellite not being able to measure methane. To minimize the emissions impacts of the experiment and to reduce costs, the September campaign included alternative-satellite releases. These were flowrates designed to be used specifically if cloud coverage at the site made it impossible for the satellite to obtain a measurement. If clouds were present at the satellite overpass time, the alternative-satellite amount was released instead. The Stanford and TADI teams made the decision to proceed with either the satellite-scale or alternative-satellite release rate within an hour of the target overpass time, given local conditions.

**Table S3.** Summary of zero releases and satellite-designated releases by week.

| Week | Number of Zero Releases | Number of Satellite Releases |
|---|---|---|
| 1 | 2 | 3 |
| 2 | 1[a] | 3 |
| 3 | 2 | 1[b] |
| 4 | 2 | 2 |

[a] *Week 2 only has 1 zero release because of the decision to cancel Friday afternoon releases.*
[b] *Week 3 only has 1 satellite release because of cloud conditions.*

Complete schedules of methane releases with release start and end times, flowrates, and uncertainties can be found in the following tables.

### S1.2.3 Methane release flowrates and schedules

**Table S4.** Week 1 methane release flowrates and times

| Week | Date | Release Start | Release end | Flowrate (kg/h) | Uncertainty (%) |
|---|---|---|---|---|---|
| 1 | 6/17/24 | 11:07:00 | 11:53:30 | 28.26 | 3.3 |
| 1 | 6/17/24 | 12:05:00 | 12:51:00 | 0.66 | 7 |
| 1 | 6/17/24 | 13:05:45 | 13:52:00 | 20 | 0.67 |
| 1 | 6/17/24 | 14:00:00 | 14:48:30 | 8.28 | 11.08 |
| 1 | 6/17/24 | 15:00:00 | 15:46:00 | 1.49 | 3.15 |
| 1 | 6/17/24 | 16:00:00 | 16:47:30 | 16.46 | 0.69 |
| 1 | 6/17/24 | 16:57:05 | 17:48:30 | 56.7 | 1.73 |
| 1 | 6/18/24 | 9:08:00 | 9:54:00 | 41 | 2.32 |
| 1 | 6/18/24 | 10:05:05 | 10:51:30 | 28.26 | 3.3 |
| 1 | 6/18/24 | 11:03:00 | 11:49:00 | 4.45 | 7.54 |
| 1 | 6/18/24 | 12:00:30 | 12:46:30 | 8.28 | 11.08 |
| 1 | 6/18/24 | 13:00:00 | 13:46:00 | 47.66 | 2.02 |
| 1 | 6/18/24 | 14:04:05 | 14:51:00 | 3.83 | 8.82 |
| 1 | 6/18/24 | 15:05:45 | 15:33:00 | 1.95 | 12.72 |
| 1 | 6/18/24 | 15:38:00 | 16:25:00 | 126 | 1.38 |
| 1 | 6/18/24 | 16:41:00 | 17:35:15 | 4.46 | 7.54 |
| 1 | 6/19/24 | 9:00:50 | 9:47:10 | 16.95 | 0.69 |
| 1 | 6/19/24 | 10:00:45 | 10:49:10 | 1.92 | 2.48 |
| 1 | 6/19/24 | 11:01:45 | 11:48:00 | 115 | 1.49 |
| 1 | 6/19/24 | 12:00:30 | 12:47:00 | 0 | 0 |
| 1 | 6/19/24 | 13:02:20 | 13:48:10 | 38.52 | 2.46 |
| 1 | 6/19/24 | 14:01:15 | 14:50:30 | 5.6 | 6.01 |
| 1 | 6/19/24 | 15:02:00 | 15:48:00 | 103.2 | 1.63 |
| 1 | 6/19/24 | 16:02:15 | 16:50:00 | 8.28 | 0.85 |

| | | | | | |
|---|---|---|---|---|---|
| 1 | 6/20/24 | 9:00:00 | 9:47:30 | 13.59 | 6.76 |
| 1 | 6/20/24 | 10:03:05 | 10:49:00 | 24.01 | 3.86 |
| 1 | 6/20/24 | 11:00:30 | 11:51:30 | 16.92 | 5.72 |
| 1 | 6/20/24 | 12:03:00 | 12:51:00 | 43.49 | 2.19 |
| 1 | 6/20/24 | 13:07:00 | 13:53:05 | 5.63 | 6.01 |
| 1 | 6/20/24 | 14:08:00 | 14:56:00 | 20 | 0.67 |
| 1 | 6/20/24 | 15:14:10 | 16:30:00 | 101.8 | 1.65 |
| 1 | 6/20/24 | 16:18:00 | 17:05:30 | 13 | 0.73 |
| 1 | 6/21/24 | 9:00:15 | 9:47:30 | 1.1 | 4.12 |
| 1 | 6/21/24 | 10:02:45 | 10:49:00 | 27.84 | 3.35 |
| 1 | 6/21/24 | 11:04:00 | 11:56:30 | 5.38 | 1.07 |
| 1 | 6/21/24 | 12:10:00 | 13:04:00 | 0 | 0 |
| 1 | 6/21/24 | 13:13:30 | 14:01:20 | 40.63 | 2.34 |
| 1 | 6/21/24 | 14:12:00 | 15:05:00 | 0.01 | 2 |
| 1 | 6/21/24 | 15:15:20 | 16:06:00 | 15.15 | 6.07 |
| 1 | 6/21/24 | 16:29:30 | 17:19:40 | 3.95 | 8.5 |

**Table S5.** Week 2 methane release flowrates and times

| Week | Date | ReleaseStart | ReleaseEnd | Flowrate (kg/h) | Uncertainty (%) |
|---|---|---|---|---|---|
| 2 | 6/24/24 | 11:08:45 | 11:55:00 | 0.59 | 7.86 |
| 2 | 6/24/24 | 12:00:00 | 12:45:00 | 136.6 | 1.29 |
| 2 | 6/24/24 | 13:02:00 | 13:45:00 | 24.83 | 3.74 |
| 2 | 6/24/24 | 14:01:25 | 14:48:30 | 0.89 | 5.07 |
| 2 | 6/24/24 | 15:01:15 | 15:53:30 | 46.2 | 2.08 |
| 2 | 6/24/24 | 16:05:15 | 16:51:00 | 19.23 | 0.68 |

| | | | | | |
|---|---|---|---|---|---|
| 2 | 6/24/24 | 17:00:15 | 17:49:00 | 32.18 | 2.91 |
| 2 | 6/25/24 | 9:02:00 | 9:48:00 | 0.77 | 6.02 |
| 2 | 6/25/24 | 10:03:00 | 10:49:00 | 1.95 | 2.43 |
| 2 | 6/25/24 | 11:05:00 | 11:51:00 | 8.2 | 11.17 |
| 2 | 6/25/24 | 12:05:00 | 12:51:15 | 32.1 | 2.92 |
| 2 | 6/25/24 | 13:35:00 | 14:21:00 | 50.42 | 1.92 |
| 2 | 6/25/24 | 14:35:00 | 15:22:00 | 21.7 | 4.26 |
| 2 | 6/25/24 | 15:33:00 | 16:19:00 | 54.95 | 1.78 |
| 2 | 6/25/24 | 16:39:00 | 17:34:30 | 1.48 | 3.15 |
| 2 | 6/26/24 | 8:55:00 | 9:43:00 | 1.62 | 2.88 |
| 2 | 6/26/24 | 10:01:00 | 10:52:00 | 1.33 | 3.47 |
| 2 | 6/26/24 | 11:00:00 | 11:50:00 | 9.71 | 0.8 |
| 2 | 6/26/24 | 13:03:10 | 13:51:10 | 4.83 | 1.15 |
| 2 | 6/26/24 | 14:00:00 | 14:52:20 | 0.01 | 2 |
| 2 | 6/26/24 | 15:01:20 | 15:49:30 | 44.02 | 2.17 |
| 2 | 6/26/24 | 16:03:00 | 16:50:00 | 8.55 | 10.71 |
| 2 | 6/26/24 | 17:01:00 | 17:47:00 | 0 | 0 |
| 2 | 6/27/24 | 8:56:00 | 9:44:00 | 37.59 | 2.51 |
| 2 | 6/27/24 | 10:09:00 | 10:55:00 | 42.06 | 2.26 |
| 2 | 6/27/24 | 11:06:00 | 11:56:30 | 0.57 | 7.86 |
| 2 | 6/27/24 | 12:09:00 | 12:55:00 | 8.55 | 10.71 |
| 2 | 6/27/24 | 13:29:00 | 14:15:00 | 13.91 | 6.62 |
| 2 | 6/27/24 | 14:35:00 | 15:22:00 | 37.59 | 2.51 |
| 2 | 6/27/24 | 15:33:15 | 16:19:15 | 81.3 | 2.01 |
| 2 | 6/27/24 | 16:35:30 | 17:24:05 | 1.44 | 3.22 |
| 2 | 6/28/24 | 9:00:00 | 9:47:30 | 2.98 | 1.67 |

| | | | | | |
|---|---|---|---|---|---|
| 2 | 6/28/24 | 10:10:40 | 10:56:00 | 0.32 | 2 |
| 2 | 6/28/24 | 11:02:30 | 11:49:15 | 189 | 1.03 |
| 2 | 6/28/24 | 12:03:30 | 12:51:00 | 19.23 | 0.68 |

**Table S6.** Week 3 methane release flowrates and times

| Week | Date | ReleaseStart | ReleaseEnd | Flowrate (kg/h) | Uncertainty (%) |
|---|---|---|---|---|---|
| 3 | 9/9/24 | 11:02:30 | 11:50:10 | 56.7 | 1.73 |
| 3 | 9/9/24 | 12:05:00 | 12:52:30 | 31.36 | 2.98 |
| 3 | 9/9/24 | 13:23:55 | 14:16:00 | 5.57 | 1.05 |
| 3 | 9/9/24 | 14:30:30 | 15:20:45 | 0 | 0 |
| 3 | 9/9/24 | 15:25:15 | 16:15:40 | 0.18 | 2 |
| 3 | 9/9/24 | 16:42:00 | 17:36:30 | 13.38 | 0.72 |
| 3 | 9/10/24 | 8:45:00 | 9:31:00 | 0.92 | 4.88 |
| 3 | 9/10/24 | 9:45:15 | 10:31:00 | 2.02 | 2.35 |
| 3 | 9/10/24 | 10:40:00 | 11:26:00 | 79.2 | 2.05 |
| 3 | 9/10/24 | 11:45:00 | 12:31:00 | 17.8 | 5.19 |
| 3 | 9/10/24 | 12:44:00 | 13:36:30 | 6.77 | 0.94 |
| 3 | 9/10/24 | 13:44:15 | 14:30:00 | 1.85 | 2.57 |
| 3 | 9/10/24 | 14:44:00 | 15:30:00 | 28.16 | 3.31 |
| 3 | 9/10/24 | 15:44:00 | 16:30:00 | 4.47 | 1.22 |
| 3 | 9/10/24 | 16:46:00 | 17:36:00 | 0.45 | 9.66 |
| 3 | 9/11/24 | 8:35:15 | 9:22:00 | 54 | 1.81 |
| 3 | 9/11/24 | 9:34:00 | 10:20:30 | 31.36 | 2.98 |
| 3 | 9/11/24 | 10:37:50 | 11:25:00 | 1.01 | 4.54 |
| 3 | 9/11/24 | 11:34:00 | 12:22:00 | 20.18 | 3.67 |

| | | | | | |
|---|---|---|---|---|---|
| 3 | 9/11/24 | 12:37:00 | 13:25:00 | 0.02 | 2 |
| 3 | 9/11/24 | 13:34:15 | 14:22:00 | 0.62 | 7.41 |
| 3 | 9/11/24 | 14:34:15 | 15:20:15 | 0.7 | 6.64 |
| 3 | 9/11/24 | 15:34:00 | 16:22:00 | 44.07 | 2.17 |
| 3 | 9/11/24 | 16:34:00 | 17:23:00 | 51.12 | 1.9 |
| 3 | 9/12/24 | 9:16:15 | 10:02:00 | 19.74 | 0.68 |
| 3 | 9/12/24 | 10:06:00 | 10:54:00 | 13.38 | 0.72 |
| 3 | 9/12/24 | 11:07:30 | 11:55:00 | 4.14 | 1.29 |
| 3 | 9/12/24 | 12:00:00 | 12:46:15 | 37.1 | 2.54 |
| 3 | 9/12/24 | 13:28:00 | 14:15:00 | 50.88 | 1.91 |
| 3 | 9/12/24 | 14:31:00 | 15:17:00 | 1.3 | 3.56 |
| 3 | 9/12/24 | 15:28:00 | 16:15:00 | 210 | 0.96 |
| 3 | 9/12/24 | 16:30:45 | 17:17:30 | 26.85 | 3.46 |
| 3 | 9/13/24 | 8:45:00 | 9:32:00 | 0 | 0 |
| 3 | 9/13/24 | 9:49:00 | 10:35:00 | 3.4 | 1.5 |
| 3 | 9/13/24 | 10:45:00 | 11:31:05 | 1.47 | 3.15 |
| 3 | 9/13/24 | 11:45:00 | 12:33:00 | 308.2 | 0.8 |
| 3 | 9/13/24 | 12:45:00 | 13:34:00 | 20.18 | 0.67 |

**Table S7.** Week 4 methane release flowrates and times

| Week | Date | ReleaseStart | ReleaseEnd | Flowrate (kg/h) | Uncertainty (%) |
|---|---|---|---|---|---|
| 4 | 9/16/24 | 11:00:00 | 11:46:10 | 0.57 | 2.21 |
| 4 | 9/16/24 | 11:59:00 | 12:47:00 | 56.7 | 1.73 |
| 4 | 9/16/24 | 12:59:00 | 13:45:00 | 11.17 | 0.76 |
| 4 | 9/16/24 | 13:59:30 | 14:46:00 | 28.71 | 3.95 |

| | | | | | |
|---|---|---|---|---|---|
| 4 | 9/16/24 | 14:59:00 | 15:45:00 | 21.64 | 4.28 |
| 4 | 9/16/24 | 15:59:00 | 16:45:00 | 9.23 | 0.81 |
| 4 | 9/17/24 | 9:00:30 | 9:46:00 | 0.9 | 5.07 |
| 4 | 9/17/24 | 9:59:00 | 10:46:00 | 7.3 | 0.9 |
| 4 | 9/17/24 | 10:59:00 | 11:50:00 | 79.2 | 2.05 |
| 4 | 9/17/24 | 11:59:30 | 12:49:30 | 5.5 | 1.06 |
| 4 | 9/17/24 | 13:00:00 | 13:46:30 | 0 | 0 |
| 4 | 9/17/24 | 13:58:30 | 14:45:00 | 54 | 1.81 |
| 4 | 9/17/24 | 14:58:00 | 15:44:00 | 0.02 | 2 |
| 4 | 9/17/24 | 15:47:00 | 16:44:00 | 44 | 2.17 |
| 4 | 9/18/24 | 8:51:30 | 9:37:00 | 0.5 | 8.97 |
| 4 | 9/18/24 | 9:44:30 | 10:31:00 | 38.47 | 2.46 |
| 4 | 9/18/24 | 10:45:00 | 11:31:15 | 1.45 | 3.22 |
| 4 | 9/18/24 | 11:44:00 | 12:33:00 | 52.94 | 1.84 |
| 4 | 9/18/24 | 12:45:00 | 13:25:30 | 0.29 | 2 |
| 4 | 9/18/24 | 13:30:00 | 14:16:00 | 8.25 | 0.85 |
| 4 | 9/18/24 | 14:29:00 | 15:15:45 | 0.19 | 2 |
| 4 | 9/18/24 | 15:30:00 | 16:17:00 | 290 | 1.67 |
| 4 | 9/18/24 | 16:31:20 | 17:19:45 | 0.73 | 6.31 |
| 4 | 9/19/24 | 8:45:00 | 9:32:30 | 28.71 | 3.25 |
| 4 | 9/19/24 | 9:45:00 | 10:31:00 | 1.63 | 2.88 |
| 4 | 9/19/24 | 10:44:00 | 11:32:00 | 2.01 | 2.35 |
| 4 | 9/19/24 | 11:44:00 | 12:31:30 | 4.14 | 1.29 |
| 4 | 9/19/24 | 12:44:00 | 13:32:30 | 49.01 | 1.97 |
| 4 | 9/19/24 | 13:46:00 | 14:34:00 | 1.14 | 3.99 |
| 4 | 9/19/24 | 14:44:00 | 15:31:00 | 80.1 | 1.67 |

| | | | | | |
|---|---|---|---|---|---|
| 4 | 9/19/24 | 15:44:30 | 16:34:00 | 8.25 | 0.85 |
| 4 | 9/19/24 | 16:44:10 | 17:36:00 | 26.4 | 3.52 |
| 4 | 9/20/24 | 8:45:15 | 9:31:00 | 3.3 | 1.53 |
| 4 | 9/20/24 | 9:45:00 | 10:34:00 | 38.47 | 2.46 |
| 4 | 9/20/24 | 10:45:00 | 11:33:00 | 34.4 | 2.73 |
| 4 | 9/20/24 | 11:46:15 | 12:33:00 | 1 | 4.54 |
| 4 | 9/20/24 | 12:46:50 | 13:33:00 | 17.93 | 0.68 |
| 4 | 9/20/24 | 13:51:00 | 14:20:00 | 0 | 0 |
| 4 | 9/20/24 | 14:32:30 | 15:20:00 | 54 | 1.81 |
| 4 | 9/20/24 | 15:32:30 | 16:41:00 | 250.8 | 0.87 |

**S1.3 Participant Scheduling**

Participant Week assignments were decided based on participant availability and test site constraints. Because the participants were going to measure concurrently, including the commercial teams, we aimed to achieve a mix of different measurement techniques in each week. Additionally, more constraints were placed on drones and aircraft. The Stanford and TADI team limited participation to two drones per week and one aircraft per week to ensure that each team had the opportunity to measure a significant number of releases while maintaining safe operations.

There were some difficulties in scheduling participants. Because the TADI site is located on a Seveso 3 industrial site, there are several restrictions and certifications placed on the operation of drones within the site and aircraft flying above it.[i] This resulted in some participants that had expressed initial interest being unable to participate in the experiment, citing difficulties with obtaining the necessary permissions for operation.

[i] SEVESO 3 industrial site refers to an industrial facility that falls under the regulations of the Seveso III Directive (Directive 2012/18/EU), meaning it handles large quantities of dangerous substances and is required to implement strict safety measures to prevent major accidents and minimize their consequences on people and the environment.

**Table S8.** Schedule of participants and the week(s) that they participated in (including commercial teams).

| Week | Vehicles | Aircraft | Drones (Commercial) | Fixed Sensors (Commercial) | Satellite (Commercial |
|---|---|---|---|---|---|
| Week 1 (June 17-21, 2024) | DTU | | Aeromon, GSMA AUSEA | Sensirion | GHGSat |
| Week 2 (June 24-28, 2024) | UHEI | | SeekOps | Sensirion | GHGSat |
| Week 3 (September 9-13, 2024) | | FAAM | | Sensirion, Sensia, SLB | GHGSat |
| Week 4 (September 16-20, 2024) | UU/LSCE/CYI/RHUL | Empa/UZH | Flylogix | Sensirion, Sensia, SLB | GHGSat |

### S1.3.1 FAAM Scheduling

In initial conversations with the FAAM team, they indicated that they would only be able participate in one day of testing. Because of the limited number of tests, the Stanford team agreed to exclude zero releases from the releases measured by FAAM. We also agreed to identify one release that would be at a scale large enough for their detection (>100 kg/h) so they could be sure to collect data from the study. This information was not made public to other teams.

## S2 Participant & Technology Descriptions

Descriptions of each participant's technology and team can be found in Sects. S2.1.1–S2.1.5. These descriptions are based on interviews conducted with each participant during their week of testing, participant submissions to technology and method surveys included with their results, and publications.

**Table S9.** Participant name, solution name, technology and sensor types, including commercial participants.

| Participant Type | Participant | Solution Name | Technology Type |
|---|---|---|---|
| Commercial | *Aeromon* | Aeromon BH-12 | Drone |
| Commercial | *GSMA* | AUSEA | Drone |
| Commercial | *Flylogix* | Flylogix Asset-level Methane emissions report | Drone |
| Commercial | *SeekOps* | TDLAS (SeekIR) Sensor | Drone |
| Commercial | *GHGSat* | GHGSat-C2, C3, C4, C5, C7, and C8 (GHGSat-C) | Satellite |
| Commercial | *Sensirion* | Nubo Sphere | Continuous Monitor |
| Commercial | *SLB* | Methane Lidar Camera | Continuous Monitor |
| Commercial | *SENSIA* | Mileva 33 | Continuous Monitor |
| Academic | *DTU* | N/A | Vehicle |
| Academic | *UHEI* | N/A | Vehicle |
| Academic | *UU/LSCE/CYI/RHUL* | N/A | Vehicle |
| Academic | *Empa/UZH* | AVIRIS-4 | Aircraft |
| Academic | *FAAM* | N/A | Aircraft |

Many of the participants in this experiment have participated in previous testing at TADI or in single-blind controlled release experiments conducted by Stanford. Previous testing may have resulted in more familiarity with the testing methods and site configuration.

**Table S10.** Previous controlled release testing of the participants.

| Solution | Previously Tested by Stanford | Previously Tested on TADI or TotalEnergies Sites |
|---|---|---|
| *DTU* | No | No |
| *UHEI* | No | No |
| *UU/LSCE/CYI/RHUL* | No | Yes (LSCE) |
| *Empa/UZH* | No | No |
| *FAAM* | No | No |

## S2.1 Description of Academic Institutions and Deployed Technology

### S2.1.1 Technical University of Denmark (DTU)

The DTU team deployed a mobile ground-based system using a 2017 van equipped with a Picarro cavity ring-down spectrometer (model G2203) that measures methane and acetylene concentrations *in situ*. The team employed a tracer gas dispersion method for emission quantification, which combines the controlled release of acetylene as a tracer gas with downwind measurements of both methane and acetylene concentrations to reconstruct plume dispersion characteristics.

The methodology involves releasing acetylene at a known, constant rate from the suspected emission source while conducting at least 10 cross-plume measurements of atmospheric methane and acetylene concentrations using the mobile platform. Air is sampled at approximately 2 m height as the vehicle traverses downwind transects. The approach assumes that methane and acetylene undergo identical dispersion and transport processes, allowing methane emission rates to be inferred from the ratio of observed methane to acetylene concentrations and the known acetylene release rate. This tracer gas dispersion method is described in detail in earlier publications and has been shown in previous controlled release studies to achieve quantification errors very likely less than 20% for fugitive emissions from area sources (Mønster et al., 2014; Delre et al., 2018; Fredenslund et al., 2019, 2023; Kissas et al., 2022). Additional details on this methodology can be found in Mønster et al. (2014) and Fredenslund et al. (2019).

For the TADI experiments, acetylene was released via tubing into the center of the ATEX zone from a gas cylinder positioned near the test site. The measurements at TADI deviated from typical operational practices in two key ways. First, the emission zone could not be surveyed beforehand to determine precise emission locations, and emission location within the platform varied and was blinded to participants, which prevented optimal tracer gas placement at or near the actual sources. Second, real-time adjustment of tracer placement based on methane-acetylene correlation during measurement – a standard practice to optimize method performance – was not possible due to the controlled experimental constraints.

The Department of Environmental and Resource Engineering (DTU Sustain) is located at the Technical University of Denmark in Copenhagen, Denmark. DTU Sustain is an academic organization focusing on developing new sustainable technologies, methods, and solutions. The department is involved in education, research, and research-based consulting services (DTU Sustain, 2025).

### S2.1.2 Heidelberg University (UHEI)

The Heidelberg University (UHEI) team deployed a mobile, ground-based measurement system using a 2019 Volkswagen van equipped with a LI-COR LI-7810 optical feedback-cavity enhanced absorption spectrometer for in situ $CH_4$ and $CO_2$ concentration measurements. The instrument has a 1σ precision of 0.25 ppb at 2 ppm with 5-second averaging. A standard gas cylinder was regularly measured throughout the five-day release campaign to ensure instrument stability. The system included dual meteorological monitoring: a fixed 3D sonic anemometer and a mobile weather station mounted near the intake line on the vehicle roof. These provided the local atmospheric data required for the emission quantification algorithms.

During mobile transects, the emission plume was crossed between 10 and 27 times per release. When wind conditions allowed, measurements were conducted during 11 releases at two different distances from the TADI platform to improve the spatial resolution of the emission estimates and their robustness. For each release, individual emission estimates were calculated per transect, and the median value was reported. In addition to the mobile measurements, stationary measurements were conducted during three controlled releases, during which $CH_4$ were recorded directly downwind, aligned with the prevailing wind direction.

Methane emission rates were calculated using two complementary approaches: 1) the Other Test Method 33a (OTM33a) protocol (Korbeń et al., 2022; Morales et al., 2022), and 2) a Gaussian plume model (Korbeń et al., 2022; Wietzel et al., 2025). The OTM33a method uses stationary measurements collected downwind of the source to estimate emissions, whereas the Gaussian plume model relies on $CH_4$ concentrations recorded during mobile transects through the emission plume. Both methods integrate site-specific meteorological data to account for atmospheric dispersion. Detailed information on the application of the OTM33a method can be found in Korbeń et al. (2022). Wietzel et al. (2025) extensively tested and evaluated the Gaussian plume modelling approach in combination with mobile measurements, including its data processing and application with release experiments. This study demonstrated that uncertainties associated with the Gaussian method can be reduced to approximately 30% when following a defined best-practice strategy.

For routine campaigns, mobile measurements are typically avoided at wind speeds below 2 m/s due to increased plume meandering under calm conditions. However, during the TADI campaign, measurements were carried out under all weather conditions, including wind speeds below 2 m/s, as the team were already on site. In approximately 40% of the release experiments, wind speeds were below 2 m/s. Measurements were still conducted and emission rates calculated but flagged as not valid for the official reporting. As result only 19 of the 34 releases, in which UHEI participated, are included in this study.

The Institute of Environmental Physics at Heidelberg University in Germany researches questions that explore the flow of energy and matter in our environment. Through investigation of the cycle of atmospheric water and greenhouse gases, Dr. Martina Schmidt's group develops methods for quantifying emissions sources (Heidelberg University, 2025).

### S2.1.3 The Cyprus Institute (CYI), Royal Holloway University of London (RHUL), Utrecht University (UU), and the Laboratory for Climate and Environmental Sciences (France) (LSCE)

In week 4 of the campaign, four academic teams collaborated on measuring methane with three different sensors mounted in a single vehicle. The methane concentration measurement devices included an ABB sensor, an Aeris MIRA Ultra methane analyzer, and a Picarro G2311-f analyzer. The vehicle also was equipped with an Airmar anemometer and GPS system. This team also installed a stationary Trisonica anemometer near the release area. The vehicle is repeatedly driven around the release area and online sensors screens are checked live to verify when the vehicle is crossing the plume. $CH_4$ concentration data from the analyzers are merged with the GPS and wind data to estimate the source location. The source-estimated location and the atmospheric stability class are used in a Gaussian Plume Dispersion Model to estimate the release rate based on the observed concentration data. Assumptions are made about the release point height.

Initially, it was planned to have separated quantification and detection results from each of the teams (CYI/LSCE, RHUL, and UU), even if they used a common vehicle and the same wind and GPS measurement devices. After the campaign concluded, they decided to provide only one common estimated emission rate for each release.

The Cyprus Institute is a research and educational institution located in Cyprus (The Cyprus Institute, 2025). Royal Holloway University of London is a research and educational institution based in the U.K. (Royal Holloway University of London, 2025). Utrecht University is a research and educational institution in the Netherlands (Utrecht University, 2025). The Laboratory for Climate and Environmental Sciences is a joint research unit between several French governmental agencies, universities, and institutes (LSCE, 2025).

### S2.1.4 Swiss Federal Laboratories for Materials Science and Technology and University of Zurich (Empa/UZH)

Emission quantification from AVIRIS-4 involves four steps (five to get one average per release):

1) Radiometric and spectral calibration: The data recorded by AVIRIS-4 consists of digital numbers (DN) with the spatial dimensions along track and across track as well as a spectral dimension consisting of 287 bands at wavelengths ranging from 375 to 2500 nm (called

level 0 data). The digital numbers are then converted into at-sensor radiances (in W $m^{-2}$ $nm^{-2}$ $sr^{-1}$) using laboratory-measured calibration coefficients $c_0$ (offset) and $c_1$ (gain): $L = c_0 + c_1 * DN$. This data is called level 1 data.

2) Georectification: Due to a defective cable, the AVIRIS-4 and GPS timestamps were not synchronized correctly during the campaign. Consequently, precise georeferencing was not yet available when reporting emissions. For this reason, a simple georectification has been applied where the data is projected onto a lat/lon grid with constant pixel sizes, where the pixel size has been estimated based on the altitude and speed of the aircraft as well as the viewing angle and FPS of the sensor. This results in an overestimation of the pixel areas by approximately 5% with a standard deviation of 6% compared to measurements in Google Earth.

3) Methane retrieval: Methane enhancements are retrieved from at-sensor radiances using a matched filter based on the implementation by Foote et al. (2020). The matched filter is applied to two spectral windows (1.6µm and 2.3µm). An albedo correction is applied independently for each window. The application of the algorithm to AVIRIS-NG is described by Kuhlmann et al. (2025). The unit absorption spectrum of methane is calculated by computing a simulated spectrum representative for mid-latitude summer conditions without methane enhancements (L0) and one with an assumed methane enhancement of 10 ppm in the lowest kilometer of the atmosphere (L1). The calculated spectra depend on the solar zenith angle and the altitude of the aircraft above ground. The unit absorption spectrum is obtained as $s = (\ln(L1) - \ln(L0)) / alpha$ where alpha = enhancement * altitude above ground. The matched filter is then applied to each across-track position to obtain methane enhancements above the background. The resulting maps of methane are called level 2 data.

4) Emission quantification: The method used for emission estimation is the Integrated Mass Enhancement (IME) method described in Kuhlmann et al. (2025). In a first step, the plumes are detected by using a threshold of the methane enhancements above the background. The source location is obtained from the high-resolution methane image. The background concentration is estimated by applying a low-pass filter (i.e. a median filter) assuming a spatially smooth background field. In a second step, the integrated mass enhancement (IME) is calculated as the sum of methane columns in each pixel multiplied with the area of each pixel. Lastly, the IME is multiplied by the residence time tau of the methane within the plume where $tau = u / L$. u represents the (effective) wind speed and L the plume length.

5) Emission estimation for each release: The data were reported as one estimate for each overpass and as one estimate for each release. For the latter, Empa/UZH calculated the estimated emissions as the weighted average of all estimates for a given release using $1/\sigma^2$ as weights where $\sigma$ is the uncertainty for one estimate. For the uncertainty of the estimated emissions per release, the median of all estimates is used for a given release instead of a weighted average because the estimated uncertainties are assumed not to be independent due to systematic errors

(e.g. for the estimation of wind speeds, pixel sizes etc.). This yields a more conservative estimate of the uncertainties which will be improved in further analyses.

The Empa/UZH team was comprised of researchers from the Laboratory for Air Pollution and Environmental Technology, a federal research institute within ETH Zurich with experts on trace gas remote sensing and atmospheric transport modeling, and researchers with the Remote Sensing Laboratory at the University of Zurich in Switzerland, who own and operate the sensor and are experts in remote sensing (Empa, 2025; University of Zurich, 2025). The aircraft was operated by Swiss Flight Services.

**S2.1.5 FAAM Airborne Laboratory**

The FAAM Airborne Laboratory is a research facility dedicated to the advancement of atmospheric science. They operate a specially adapted BAe-146-301 Atmospheric Research Aircraft and are based at Cranfield University and Airfield (FAAM, 2025).

Position data (latitude, longitude, altitude, ground speed, heading) are provided by a GPS-aided inertial navigation system (GIN). A full description of the meteorological measurements' capability (temperature, humidity, winds) is provided in Price (2022).

Gas-phase in-situ chemistry measurements are conducted for greenhouse gases ($CO_2$, $CH_4$ and $H_2O$) using a customized Los Gatos Research Inc. Fast Greenhouse Gas Analyzer (model 907-011-000-000), based on the laser absorption off-axis integrated cavity output spectroscopy technique. The methods for 1 Hz measurement, initially flown in 2011, are described in O'Shea et al. (2013). The FGGA system was subsequently upgraded in 2019 and 2021 to measure gas mole fractions in dry air at 10 Hz (Shaw et al., 2022). Reported CH4 mole fractions are linearized using in-flight calibrations by overflowing the aircraft inlet (for 45 seconds) with known "low" and "high" near ambient mole fractions of CH4 in dry natural air, at ~45 minutes interval. The 10 Hz measurements systematic bias, 1-sigma accuracy and precision are further checked in-flight by performing randomized "target" calibrations, whereby the reported linearized "target" mole fractions are compared to the known "target" mole fraction of the calibration gas. Fig. S3 shows the Gaussian fitted 10 Hz equilibrated target mole fractions (6622 data points) reported for six science missions flown by FAAM between 10 June and 25 October 2024. Data for the single mission flown during the TADI controlled release of 12 September 2024 has been highlighted by the dashed box. For 2024, the Gaussian fit analysis reveals a negligible negative CH4 measurement bias (-0.56 ppb), and a 1-sigma precision for 10 Hz measurements of 2.2 ppb. The equivalent analysis for 10 Hz CO2 "target" measurements confirmed a negligible bias of 0.02 ppm and a 1-sigma precision of 0.55 ppm.

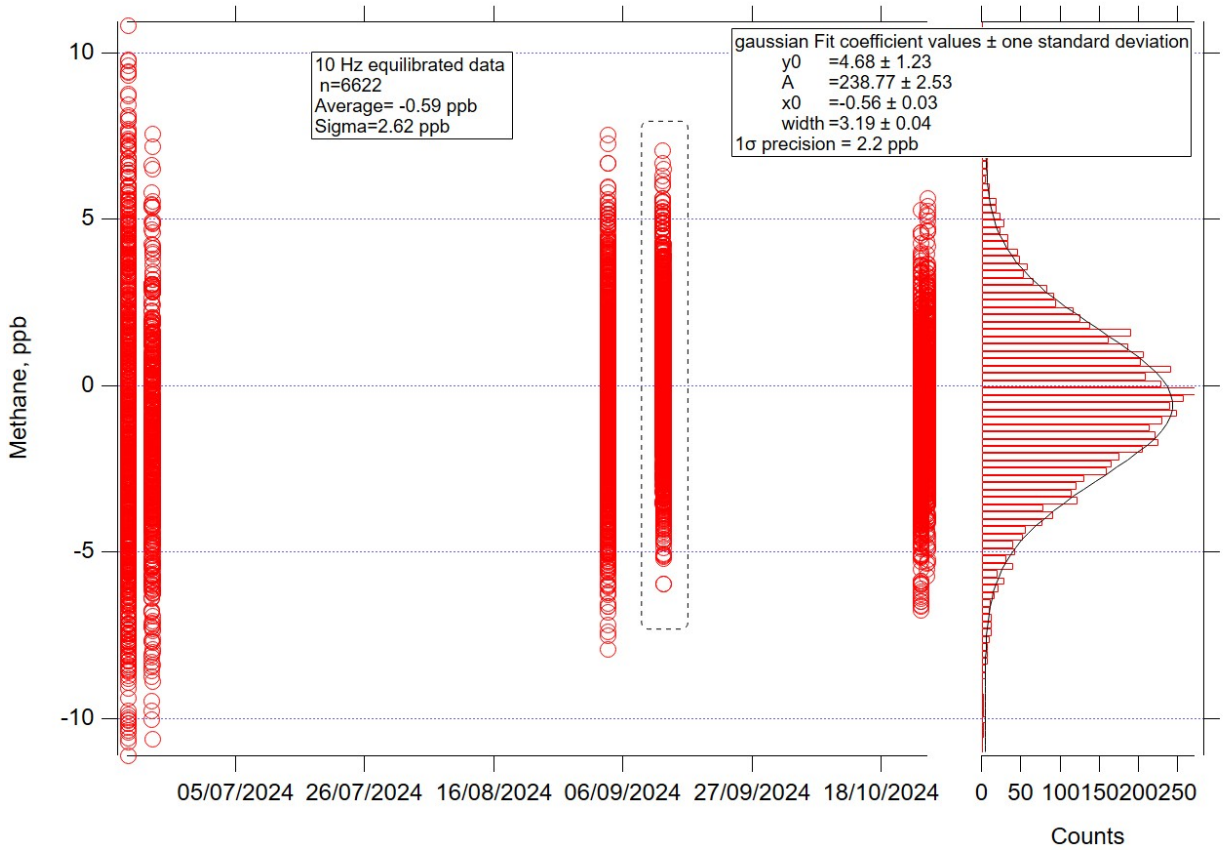



**Figure S3.** Performance in-flight "target" measurements for six missions flown in 2024 (two in June, two in September, two in October) to determine 10 Hz $CH_4$ measurements bias and precision. The dashed box indicates the data obtained during the TADI controlled release experiment on 12 September.

The 1-sigma overall uncertainty is derived by combining (using quadrature root sum square) uncertainties associated with the 10 Hz precision, the standard deviation of residuals of quadratically fitted water vapor experimental data used to derive mole fractions in dry air (as described in O'Shea et al., 2013), and the uncertainty of the mole fraction of the EMPA-certified cylinder for "target" calibrations. The 1-sigma overall uncertainties based on in-flight calibrations are ± 0.67 ppm for CO2 and ± 3.7 ppb for CH4. Measurements are traceable to the World Meteorological Organization greenhouse gases scales WMO-CO2-X2019 and WMO-CH4-X2004A.

The FGGA inlet lag time is 175±46 ms, and the instrument e-fold flush time is 140±46 ms. Both were quantified experimentally by repeatedly flushing the aircraft inlet with nitrogen with a fast-acting solenoid valve and monitoring the signal response speed.

Carbon monoxide mole fractions are measured at 1 Hz by an Aero-Laser GmbH VUV resonance fluorescence spectrometer (model AL5005). This instrument shares the same inlet and calibration system as the FGGA. Measurements are traceable to the World Meteorological Organization greenhouse gases scale WMO-CO-X2014A.

Ozone mole fractions are measured every 2 secs with a 2B Technologies Inc. dual beam UV absorption photometer (see full description of model 205; Bauguitte, 2023).

Nitrogen oxides (NO and $NO_2$) are measured at 10 Hz by a fast dual channel chemiluminescence analyzer developed collaboratively with NOAA and Air Quality Design Inc. Two detector channels operate in parallel and share a common pressure-controlled inlet allowing for parallel calibration. The inlet design follows a bypass design similar to that described in Pollack et al. (2010). A chemiluminescent zero is taken every ~5 min by increasing the NO + O3 reaction time as in Drummond et al. (1985) in 240 mL PFA Teflon zero volumes. The chemiluminescence reaction volumes are temperature controlled and follow the 241 mL gold plated design of Ridley and Grahek (1990). To mitigate sensitivity drift due to chemiluminescence quenching by water, the reagent ozone is humidified to 2-3% as in Ridley and Grahek (1990).

Sulphur dioxide mole fractions are measured at 1 Hz using a customized Thermo Fisher Scientific pulsed UV fluorescence analyzer (see full description of model TEi43i TLE; Bauguitte, 2022).

Discreet ethane and other non-methane hydrocarbons are measured off-line by collaborators at the University of York, Wolfson Atmospheric Chemistry Laboratories. GC-FID/MS analysis was performed on 80 pressurized stainless steel canisters collected during the mission (University of York, 2026).

Discreet $\delta^{13}C_{CH4}$ ($^{13}C$:$^{12}C$ stable $CH_4$ isotopes ratio) are measured off-line by collaborators at the Royal Holloway University of London, Earth Sciences Department's Greenhouse Gas Laboratory. Methane isotopic analysis by GC-Continuous Flow-Mass Spectrometry was performed on 18 Tedlar bags collected during the mission (Royal Holloway University of London, 2026).

Gas-phase chemistry measurements are further complemented by aerosol number concentrations provided by a Passive Cavity Aerosol Spectrometer Probe (PCASP) with SPP-200 electronics, operated in a wing-mounted canister. This instrument provides aggregated 10 Hz particle numbers in 30 size bins across a nominal diameter range of 0.1–3 µm. The smallest bin is discarded due to an undefined lower boundary, and bins are merged at the gain-stage crossover points as described by Ryder et al. (2013). Particles are binned according to the strength of the photovoltage generated by the HeNe laser light scattered by each particle. Laboratory calibrations both before and after the campaign are used to convert photovoltages into scattering cross-sections for each bin (Rosenberg et al., 2012).

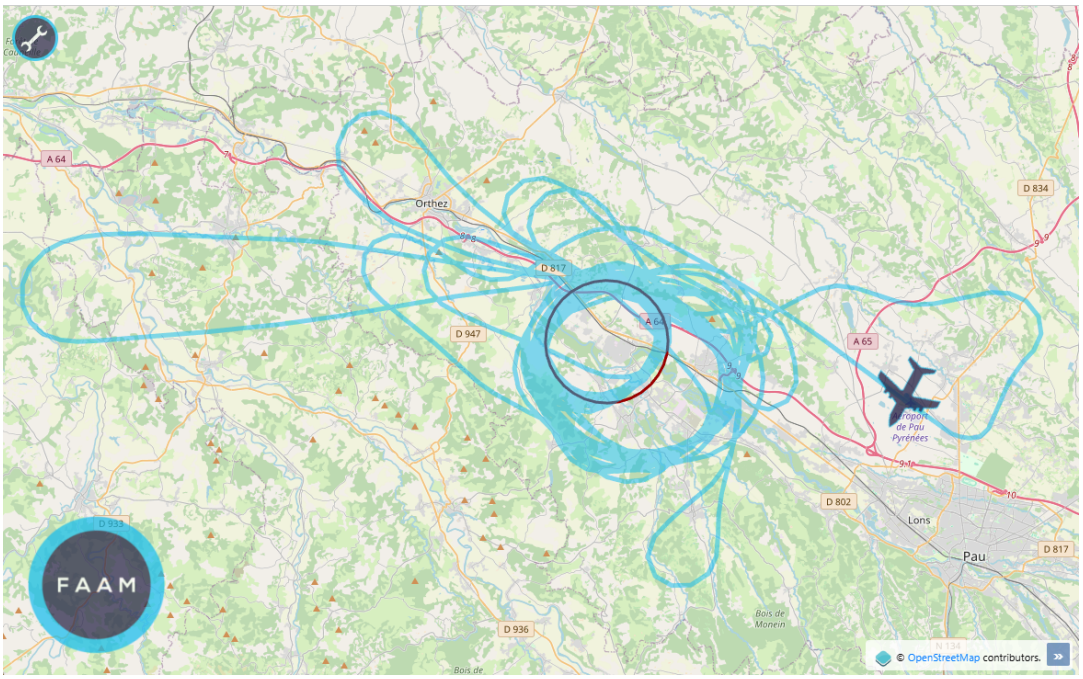



Figure S4. Flight-track of the FAAM aircraft during mission C388 (12 September 2024). The 2 NM radius red circle is centered around the TADI facility.

A total of 40 orbits were flown between 12:03 and 15:33 (UTC). Given the release start/stop local (UTC+2) times for week 3, 12 September 2024, in Table S6, the FAAM aircraft may have sampled part of the advected plume from release 5, as well as release 8, and was definitely on task for releases 6 and 7. The low and unbroken cloud cover which prevented our morning mission was still dissipating by the time we took off, and precipitation and poor visibility still affected our mission during controlled release 6. The tighter orbits flown along the 2 NM radius circuit (red circle in Fig. S4) were flown during release 7, to ensure good statistical sampling as agreed with the TADI team (see Sect. S1.3.1).

FAAM data were merged to a common 10 Hz time base, with chemistry measurements timestamps corrected for time lags. Multiple plumes were detected from sources originating within and around the IndusLacq complex, including the A64/E80 motorway. Combustion sources were identified from chemical markers such as $NO_x$, $CO_2$, $SO_2$ and aerosols (PCASP). Matlab plots were generated to establish the geographical extent of plumes detected during orbits, and their chemical fingerprint. We did not find evidence of our aircraft exhaust (effectively a continuous line source) advecting in the task area during orbits and compromising the validity of our measurements.

The detected $CH_4$ plumes were well resolved by our in-situ spectrometer as shown in Fig. S5.

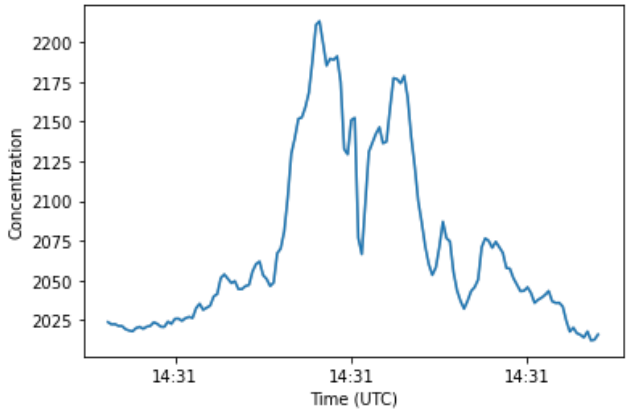



Figure S5. Example of $CH_4$ plume (10 Hz resolution) detected between 14:31:18.8 and 14:31:32.0 UTC at 191 m above ground level

Methane and other chemical tracers were identified during orbits as exemplified in Figs. S6 and S7. The heat maps and timeseries of $CH_4$ and $CO_2/NO_2/SO_2$ indicate a secondary combustion source plume being detected. The geo-temporal differentiation of the TADI-emitted $CH_4$ and combustion plumes is therefore critical in ensuring the correct plume is being integrated; in this instance the spatially broader combustion plume precedes the narrower $CH_4$ plume during our airborne sampling. This illustrates the challenge faced by airborne operators tasked in detecting and accurately quantifying emissions, critically if airborne operators do not have instrumented payload capable of multiple in-situ chemical measurements.

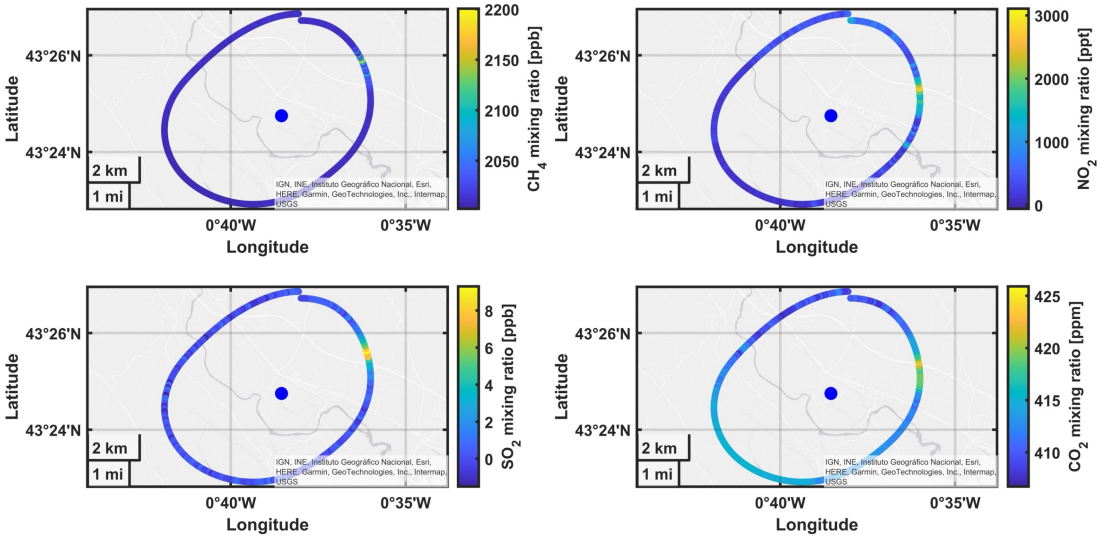



Figure S6. Heat maps of CH4, SO2, NO2 and CO2 mole fractions during an anticlockwise orbit around TADI site

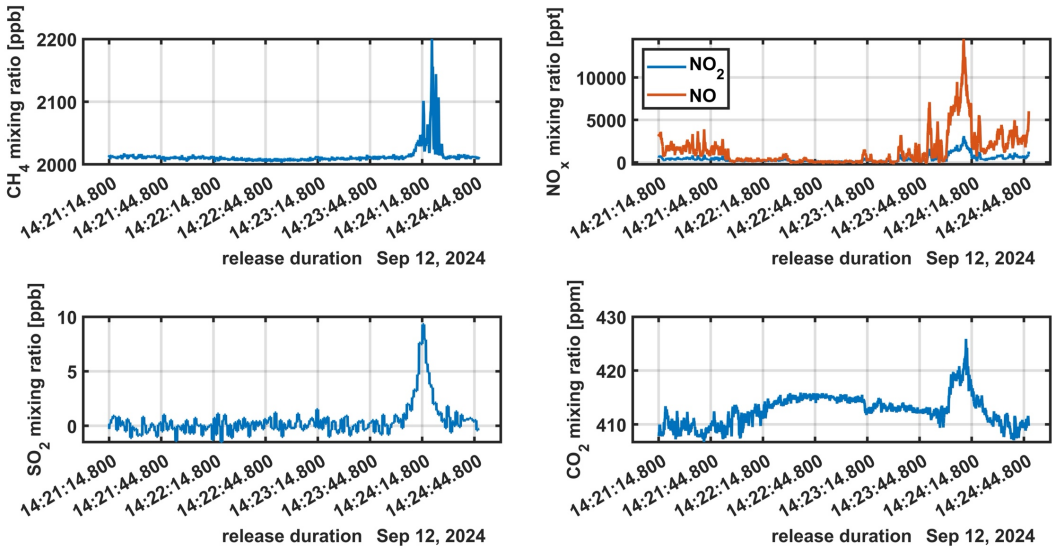



Figure S7. Timeseries of $CH_4$, $SO_2$, $NO_2$ and $CO_2$ mole fractions during an anticlockwise orbit around TADI site

Discreet VOC measurements from whole air samples (pressurized canisters) did not reveal significant ethane enhancements in the detected plumes, with ethane concentrations between 1 and 2 ppb.

Of the 8 Tedlar bags collected in plumes detected during controlled release 7, 4 samples yielded sufficient $CH_4$ enhancements above background concentrations to allow for Keeling plot calculations, resulting in $\delta^{13}C_{CH4}$ isotopic signature ranging -40.77 to -45.68‰. These values compare to -41.81‰ for 2 high $CH_4$ concentration samples collected on the ground during TADI releases by Royal Holloway personnel from the UU/LSCE/CYI/RHUL team (week 4) and provide further confidence that the correct fossil fuel release plumes were identified.

$CH_4$ plume start/stop times were defined manually for each orbit, based on the absence of combustion chemical tracers and aerosols. This was necessary given the complexity of deconvoluting multiple plumes with differing baselines; a task that was beyond the capability of our automated Python script analyzing the variance of an upwind baseline and detecting the downwind divergence above defined standard deviations.

Each orbit $CH_4$ plume enhancements were integrated to obtain ppb.s values using a Python script and scaled to ppb.m using the mean aircraft ground speed measured by GIN (112±3 m/s), to obtain *Observed Integrated $CH_4$ Enhancements*.

A new quantification methodology developed by FAAM consists of simulating a methane dispersion using the ADMS6 model to generate a concentration enhancement field in a grided domain (10 x 10 km centered on TADI-PPL, 10 m resolution in XY plane) (CERC, 2026). The model is optimized for the meteorology measured by our aircraft (temperature, wind speed and

direction). The boundary layer height is determined during ascent and descent profiles using Tephigrams and in-situ $H_2O$, $CO_2$ and $O_3$. A single point source is assumed (centered on TADI-PPL), the characteristics of which are also estimated.

An *Initial Emission Rate* [e.g. 100 g/s] is simulated to obtain dispersed methane enhancements at 11 elevations (50 to 450 m) above ground level.

The flight track of observed plumes is projected in the ADMS6 model domain, by ensuring the aircraft GIN latitude/longitude are first re-projected from their World Geodetic System 1984 (WGS 84) ellipsoid coordinate system onto the French RFG93 Lambert-93 coordinate system used for the ADMS6 domain. The aircraft GIN altitude is referenced to the TADI elevation and matched to the cubic spline-interpolated modelled elevation above the TADI site. The dispersion modelled $CH_4$ enhancements are integrated in a similar fashion as the observed $CH_4$ enhancements, to obtain *Modelled Integrated $CH_4$ Enhancements* [ppb.m].

The *estimated emission rate* is then obtained by scaling the *initial emission rate* with *Observed Integrated $CH_4$ Enhancement / Modelled Integrated $CH_4$ Enhancement*.

$CH_4$ enhancements should ideally be integrated in the vertical to obtain a surface integrated enhancement [ppb.m2]. However, the altitude levels sampled by our aircraft are limited to 150 m above ground level (this air safety restriction is lifted when operating offshore with a minimum safe altitude over oceans of 30 m). Due to the scarcity of altitudinal observations during our onshore survey, we instead report "instantaneous" emission rates derived for seven intercepted plume and estimate a mean emission rate and corresponding (1σ) standard deviation for controlled release 7.

### S2.2 Flight Operator Descriptions

Some participants used contractors to pilot their operations. Below finds the description of these contract flight operators.

#### S2.2.1 Swiss Flight Services

Swiss Flight Services SA is a private Swiss company based in Colombier that operates its own fleet under the authority of the Swiss Federal office of Civil Aviation. They are an experienced service provider for aerial surveys such as photogrammetry, laser scanning, and remote sensing in general (Swiss Flight Services, 2025). Swiss Flight Services flew the Empa/UZH sensor.

### S2.3 Participant Technology Survey Responses

This section contains descriptions of the participants as reported in the Data Reporting Template spreadsheet.

## S2.3.1 DTU Technology Survey Responses

| | |
|---|---|
| Company | Technical University of Denmark - Department of Environmental and Resource Engineering |
| Product name | Tracer gas dispersion measurement of total methane emission (Acronym: TDM) |
| (1) Please provide a detailed description of system configuration and primary components including the sensor and deployment platform. Additionally, the location (latitude, longitude, height) of auxiliary components such as meteorological station or any other equipment installed at or near the Test Center must be recorded. | Deployment: Vehicle (commercial van) containing gas analyzer, air sampling pump and tubing, GNSS receiver and antenna, screen to monitor measurement results in near real time.<br><br>Auxiliary components: 21 l Acetylene ($C_2H_2$) tracer gas bottles (1 in use per measurement at TADI) fitted with reduction valve, flow adjustment valve and variable area flowmeter. A scale was used to measure tracer gas release. |
| (2) Please record the model number of each primary component in (1), if applicable. | Gas analyzer: Cavity Ring Down Spectrometer, Picarro model G2203 $CH_4/C_2H_2$ gas analyzer<br>GNSS receiver and antenna: Hemisphere R330<br>Variable area flowmeter: Brooks, model#: 1355GAE3ABJG1AAA<br>Scale: Kern & Sohn DE 60K1D |
| (3) Please record the software revision installed on the components in (1), including performer-specific software components, revisions, or customizations | Picarro: CRDS Software, version g2000 - 1.7.0.73 |
| (4) Please record the revision number of any software analytics installed offsite. For example software to convert concentration maps to mass emission quantification estimates during the experiments. | OriginPro 2023<br>Microsoft Excel 2016 |
| (5) Please provide a detailed description of the methodology used during emission detection/quantification surveys. | Continuous release of acetylene tracer gas combined with cross plume measurements (at least ten) of methane and acetylene atmospheric concentrations. Measurements are performed using a vehicle, where air is sampled at about 2m height. Tracer gas is released at the emission source at a known, constant rate.<br><br>More details in these references: (Mønster et al., 2014; Fredenslund et al., 2019)<br><br>Measurements at TADI differed from usual practise. Normally, the emission zone is surveyed to determine from where, emissions occur. This is done to ensure tracer gas is released at/near the source(s). This was not possible at TADI. Also, adjustment of tracer placement is sometimes done, if poor correlation of the two gases are seen during measurement. This was also not possible at TADI.<br><br>Please note our quality assessment of each release sent earlier. |
| (6) Please provide the confidence level at which emission detection data are reported. (e.g., 95% CI, +/- 1 sigma) | 95% CI, standard error of the mean |

| | |
|---|---|
| (7) Please record the number of personnel participating in the surveys and their roles. Any remote personnel participating in the survey in any fashion should be documented as part of the survey team in this section. Names of individual personnel are not required. | Measurement: 1 person, tracer gas release: 1 person - 2 persons in all.<br><br>At small sites, 1 person is sufficient to perform measurements. |
| (8) For hyperspectral technologies, describe how plume length is determined for quantification. | n/a |
| (9) If wind speed is used in computing total emission rate, please describe how the wind estimate is obtained, including the precise instrument or wind reanalysis product used. | n/a |
| (10) If uncertainty is reported, where is it coming from? Is it from calculations, reported data, experimentation, etc. | Here, we report measurement variability as standard error of the mean. Measurement error of the method was the subject of this reference that included controlled release tests (Fredenslund et al., 2019). |

## S2.3.2 UHEI Technology Survey Responses

| | |
|---|---|
| University | Heidelberg University (UHEI) |
| Product name | |
| (1) Please provide a detailed description of system configuration and primary components including the sensor and deployment platform. Additionally, the location (latitude, longitude, height) of auxiliary components such as meteorological station or any other equipment installed at or near the Test Center must be recorded. | inlet height: 2.7 m above ground<br>delay time: 13 seconds<br>tubing: Teflon tubing 1/4``<br>analyser: LI-7810 (LI-COR)<br>mobile weather station: 2D anemometer (MaxiMet GMX500, Gill Instruments)<br>stationary weather station: 3D ultrasonic anemometer (USA-1, METEK)<br>GPS: (BasicAirData, Google Commerce Ltd.) |
| (2) Please record the model number of each primary component in (1), if applicable. | LI-7810 (TG10-01800) |
| (3) Please record the software revision installed on the components in (1), including performer-specific software components, revisions, or customizations | |
| (4) Please record the revision number of any software analytics installed offsite. For example software to convert concentration maps to mass emission quantification estimates during the experiments. | |
| (5) Please provide a detailed description of the methodology used during emission detection/quantification surveys. | see Korbeń et al. (2022)<br><br>and Wietzel et al. (2025) |

| | |
|---|---|
| (6) Please provide the confidence level at which emission detection data are reported. (e.g., 95% CI, +/- 1 sigma) | SD/sqrt(N) |
| (7) Please record the number of personnel participating in the surveys and their roles. Any remote personnel participating in the survey in any fashion should be documented as part of the survey team in this section. Names of individual personnel are not required. | survey team: 4 (always 1 driver, 1 writer)<br>evaluation: 1 |
| (8) For hyperspectral technologies, describe how plume length is determined for quantification. | |
| (9) If wind speed is used in computing total emission rate, please describe how the wind estimate is obtained, including the precise instrument or wind reanalysis product used. | anemometer provides 1 Hz wind data; wind speed over each transect is averaged |
| (10) If uncertainty is reported, where is it coming from? Is it from calculations, reported data, experimentation, etc. | uncertainty is given as standard error of the median (standard deviation/sqrt(number of transects)) |

## S2.3.3 UU/LSCE/CYI/RHUL Technology Survey Responses

| | |
|---|---|
| Company | LSCE-CYI-RHUL-UU (Universities) |
| Product name | Does not apply |
| (1) Please provide a detailed description of system configuration and primary components including the sensor and deployment platform. Additionally, the location (latitude, longitude, height) of auxiliary components such as meteorological station or any other equipment installed at or near the Test Center must be recorded. | Vehicle equipped with methane analyzers (ABB, Aeris MIRA Ultra, PICARRO G...), Airmar anemometer and GPS system. Trisonica anemometer installed near the release area |
| (2) Please record the model number of each primary component in (1), if applicable. | |
| (3) Please record the software revision installed on the components in (1), including performer-specific software components, revisions, or customizations | |

| | |
|---|---|
| (4) Please record the revision number of any software analytics installed offsite. For example software to convert concentration maps to mass emission quantification estimates during the experiments. | |
| (5) Please provide a detailed description of the methodology used during emission detection/quantification surveys. | The vehicle is repeatedly driven around the release area, online sensors screen are checked live to verify when the vehicle is crossing the plume. CH4 concentration data from the analyzers are merged with the GPS and wind data to estimate the source location. The source estimated location and the atmospheric stability class are used in a Gaussian Plume Dispersion Model to estimate the release rate based on the observed concentration data. Assumptions are made about the release point height. |
| (6) Please provide the confidence level at which emission detection data are reported. (e.g., 95% CI, +/- 1 sigma) | |
| (7) Please record the number of personnel participating in the surveys and their roles. Any remote personnel participating in the survey in any fashion should be documented as part of the survey team in this section. Names of individual personnel are not required. | 4 people one site. Each participant covered all roles: driver, co-pilot (and live CH4 data stream viewer), control room. |
| (8) For hyperspectral technologies, describe how plume length is determined for quantification. | |
| (9) If wind speed is used in computing total emission rate, please describe how the wind estimate is obtained, including the precise instrument or wind reanalysis product used. | Wind data are collected by two instruments: one Airmar anemometer installed on the roof of the vehicle and one Trisonica anemometer installed near the release area |

## S2.3.4 Empa/UZH Technology Survey Responses

| | |
|---|---|
| Company | Empa/UZH |
| Product name | AVIRIS-4 |
| (1) Please provide a detailed description of system configuration and primary components including the sensor and deployment platform. Additionally, the location (latitude, longitude, height) of auxiliary components such as meteorological station or any other | The instrument is an imaging spectrometer called Airborne Visible and Infrared Imaging Spectrometer (AVIRIS-4) and was developed and built by NASA JPL and operated by the University of Zurich (UZH). AVIRIS-4 is mounted on a GSM 4000 stabilization mount to stabilise the sensor and compensate for the aircraft's movements. To be able to georeference the acquired data, the iXblue Atlans A7 inertial navigation system (INS) records the exact position and attitude of the aircraft based on the GPS signal received by the airplane's antenna and based on the acceleration in three dimensions. |

| | |
|---|---|
| equipment installed at or near the Test Center must be recorded. | The sensor is controlled from an on-board Linux station using a custom UI and the data is stored on SSD in a storage rack.<br>The sensor is built into the aft hatch of a Cessna 208B Grand Caravan EX. |
| (2) Please record the model number of each primary component in (1), if applicable. | Imaging spectrometer: AVIRIS-4<br>Gyro stabilization mount: SOMAG Gyro Stabilization Mount GSM 4000<br>INS: iXblue Atlans A7 |
| (3) Please record the software revision installed on the components in (1), including performer-specific software components, revisions, or customizations | The workstation runs on the Debian distribution.<br>Topoflight is used for flight planning and navigation during the flight. |
| (4) Please record the revision number of any software analytics installed offsite. For example software to convert concentration maps to mass emission quantification estimates during the experiments. | Emit-sds v1.4.2 by NASA JPL for radiometric and spectral calibration (https://github.com/emit-sds/emit-sds-l1b)<br>PARGE by ReSe Applications for georeferencing (version 4.1, Build 11) (not used for this study)<br>EMPA/UZH CH4 Retrieval Algorithm (git revision number: v1.0)<br>Python library for data-driven emission quantification (ddeq; Version 1.0, git revision number: v0.1.0-378-gd330966) |
| (5) Please provide a detailed description of the methodology used during emission detection/quantification surveys. | Emission quantification from AVIRIS-4 involves four steps (five to get one average per release):<br><br>1) Radiometric and spectral calibration<br>The data recorded by AVIRIS-4 consists of digital numbers (DN) with the spatial dimensions along track and across track as well as a spectral dimension consisting of 286 bands at wavelengths ranging from 400 to 2500 nm (called level 0 data). The digital numbers are then converted into at-sensor radiances (in W m-2 nm-2 sr-1) using laboratory-measured calibration coefficients c0 (offset) and c1 (gain): L = c0 + c1 * DN. This data is called level 1 data.<br><br>2) Georectification<br>Due to an issue with the INS, we were not yet able to georeference the data. As soon as the issue has been resolved, we will reprocess the data.<br>For now, a simple georectification has been applied where the data is projected onto a lat/lon grid with constant pixel sizes, where the pixel size has been estimated based on the altitude and speed of the aircraft as well as the viewing angle and FPS of the sensor. With this method, we overestimate the pixel areas by approximately 5% with a standard deviation of 6% compared to measurements in Google Earth.<br><br>3) Methane retrieval<br>Methane enhancements are retrieved from at-senor radiances using a matched filter based on the implementation by Foote et al. (2020). The matched filter is applied to two spectral windows (1.6µm and 2.3µm). An albedo correction is applied indepdently for each window. The application of the algorithm to AVIRIS-NG is described by Kuhlmann et al. 2024 (EGUSphere, submitted to ACP).<br><br>The unit absorption spectrum of methane is calculated by computing a simulated spectrum representative for mid-latitude summer conditions without methane enhancements (L0) and one with an assumed methane enhancement of 10 ppm in the lowest kilometer of the atmosphere (L1). The calculated spectra depend on the solar zenith angle and the altitude of the aircraft above ground. The unit absorption spectrum |

| | |
|---|---|
| | is obtained as s = (ln(L1) - ln(L0)) / alpha where alpha = enhancement * altitude above ground.<br><br>The matched filter is then applied to each across-track position to obtain methane enhancements above the background. The resulting maps of methane are called level 2 data.<br><br>4) Emission quantification<br>The method used for emission estimation is the Integrated Mass Enhancement (IME) method described in Kuhlmann et al. (2024).<br>In a first step, the plumes are detected by using a threshold of the methane enhancements above the background. The source location is obtained from the high-resolution methane image. The background concentration is estimated by applying a low-pass filter (e.g., a median filter) assuming a spatially smooth background field.<br>In a second step, we sum the product of methane concentrations above the background and the pixel size of all detected plume pixels to obtain the integrated mass enhancement (IME).<br>Lastly, the IME is multiplied by the residence time tau of the methane within the plume where tau = u / L. u represents the (effective) wind speed (see (9)) and L the plume length (see (8)).<br><br>5) Emission estimation for each release<br>The data is reported as one estimate for each overpass (see sheet "Reported Data") and as one estimate for each release (see sheet "Reported Data Avg". For the latter, we calculated the estimated emissions as the weighted average of all estimates for a given release using 1/sigma**2 as weights where sigma is the uncertainty for one estimate. For the uncertainty of the estimated emissions per release, we use the median of all estimates for a given release instead of a weighted average because the estimated uncertainties are assumed not to be independent due to systematic errors (e.g. for the estimation of wind speeds, pixel sizes etc.). This yields a more conservative estimate of the uncertainties which will be improved in further analyses. |
| (6) Please provide the confidence level at which emission detection data are reported. (e.g., 95% CI, +/- 1 sigma) | The confidece levels are calculated as +/- 1 sigma |
| (7) Please record the number of personnel participating in the surveys and their roles. Any remote personnel participating in the survey in any fashion should be documented as part of the survey team in this section. Names of individual personnel are not required. | Before the mission:<br>- 2 people for flight planning (obtaining permissions, planning of flight patterns and altitude etc.)<br><br>During the mission:<br>- 2 pilots, 3 participants to monitor the senor and write the log book. As soon as the sensor is fully tested and all possible errors have been corrected, it will also be possible to fly with only 2 participants.<br><br>After the mission:<br>- 1 person for processing the data from level 0 to level 1<br>- 1 person for processing the data from level 1 to level 2 and for emission estimation |
| (8) For hyperspectral technologies, describe how plume length is determined for quantification. | The plume length is calculated by fitting a center line to the detected plume using a second order spline. The arc lenght of this center line is then used as the plume length. The plume is detected by using a threshold value which is determined for each overpass |

| | |
|---|---|
| | individually to restrict the detected plume to areas without visual artifacts (e.g. cast shadows). |
| (9) If wind speed is used in computing total emission rate, please describe how the wind estimate is obtained, including the precise instrument or wind reanalysis product used. | For the wind estimate, we use the ERA-5 reanalysis product 10m wind speed as well as the ensemble model spread of the 10m wind speed. The wind data is then temporally and spatially interpolated to the time and source of the release. |
| (10) If uncertainty is reported, where is it coming from? Is it from calculations, reported data, experimentation, etc. | The uncertainty of the estimated emissions is obtained by performing error propagation of the individual sources of uncertainty. We use an uncertainty for …<br>- pixel size (sigma_A) which is estimated as 10% of the average pixel size,<br>- plume length (sigma_L) which is estimated as 10% of the plume length,<br>- CH4 columns (sigma_CH4) which is estimated as the standard deviation of the pixels outside the emission plume<br>- wind speed (sigma_U) which is estimated as the combined uncertainty of the ERA-5 model spread and an uncertainty of the effective wind speed (the wind speed at which the plume is effectively transported, depending on the emission height and atmospheric stability). The latter is estimated from large eddy simulations (LES) using the CFD model MicroHH (van Heerwaarden et al., 2017) and is equivalend to 16% of the 10m wind speed for neutral and unstable conditions.<br><br>We do not include an uncertainty term for uncertainties of the IME approach such as the assumption of steady-state conditions. We expect that this would roughly double the uncertainty estimated from the algorithm. |

## S2.3.5 FAAM Technology Survey Responses

| | |
|---|---|
| Company | FAAM Airborne Laboratory, National Centre for Atmospheric Science, University of Leeds |
| Product name | Methane emission rate |
| (1) Please provide a detailed description of system configuration and primary components including the sensor and deployment platform. Additionally, the location (latitude, longitude, height) of auxiliary components such as meteorological station or any other equipment installed at or near the Test Center must be recorded. | See Sect. S2.1.5 |
| (2) Please record the model number of each primary component in (1), if applicable. | GIN model: Applanix POS AV 410. FGGA model: 907-011-000-000, serial number US4300170500001392 (flow and pressure control customised). CO instrument model AL5005, serial number 127. Ozone instrument model 205, serial number 1034DB. NOx instrument (custom-built). Sulphur dioxide instrument model TEi43i-TLE, serial number 1505564557 (flow control customised). |

| | |
|---|---|
| (3) Please record the software revision installed on the components in (1), including performer-specific software components, revisions, or customizations | All components in (1) use their manufacturer's proprietary software. |
| (4) Please record the revision number of any software analytics installed offsite. For example software to convert concentration maps to mass emission quantification estimates during the experiments. | Aircraft data: FAAM core netcdf data file (v005) is produced using a post-processing Python suite as described in https://www.faam.ac.uk/sphinx/coredata/. FAAM core cloud physics netcdf data file (in particular 10 Hz PCASP, v602) is produced using a separate post-processing Python script. FAAM FGGA data (CH4, CO2, H2O) NASA-Ames data file is produced using Wavemetrics Igor Pro (v7.0.8.1 Build 31118) and post-processing routines v2.3. Dispersion modelling simulations were performed using CERC's ADMS version 6 and its built-in Mapper tool. We use Python v3.11.7, Matlab r2023a, Igor Pro v7 libraries and scripts for further data manipulation, such as 10 Hz common timebase data sets merging, plume detection and mole enhancement integration, coordinate systems conversion (GIN lat/long flight track to ADMS X/Y dispersion domain). |
| (5) Please provide a detailed description of the methodology used during emission detection/quantification surveys. | See Sect. S2.1.5 |
| (6) Please provide the confidence level at which emission detection data are reported. (e.g., 95% CI, +/- 1 sigma) | 1 sigma sdev |
| (7) Please record the number of personnel participating in the surveys and their roles. Any remote personnel participating in the survey in any fashion should be documented as part of the survey team in this section. Names of individual personnel are not required. | Survey staff: pilot-captain, co-pilot, 3rd-pilot (observer/ATC), cabin crew (safety) member, mission scientist, flight manager, aerosol/cloud physicist, in-situ chemistry participant 1 (also sWAS grab sampling), in-situ chemistry participant 2 (also Tedlar bag grab sampling). Survey support staff: flight operations planner (Airtask). Support data scientist (FAAM post-processing). Support sWAS canisters ethane GC off-line analysis (York). Support Tedlar bags delta13CH4 off-line analysis (Royal Holloway) |
| (8) For hyperspectral technologies, describe how plume length is determined for quantification. | not applicable |
| (9) If wind speed is used in computing total emission rate, please describe how the wind estimate is obtained, including the precise instrument or wind reanalysis product used. | Wind speed (and direction) are measured by the FAAM aircraft and used for the ADMS dispersion simulation initialisation (set as 200 m above ground level). |
| (10) If uncertainty is reported, where is it coming from? Is it from calculations, reported data, experimentation, etc. | Uncertainty expressed as statistical spread around mean. Time limitation prevented a full assessment of uncertainties (eg ADMS sensitivity, plume overlap impact on integrals), although we have ascertain some of these in a previous off-shore oil and gas platform (Elgin) study, for instance the treatment of wind and non-linearity (quote Irene's thesis) |

## S3 Field Data Collection

### S3.1 Field Data Collection Procedures

Information about release flowrate, location, start and end time was recorded onsite by the site engineer. Deviations from the schedule were recorded by hand on the printed schedule and by the Stanford team. For each release, the input flowrate and associated uncertainty was recorded. The TADI site personnel delivered this information to the Stanford team after the completion of each week.

Weather conditions, temperature, and prevailing windspeed and direction was recorded on site every morning and afternoon. Wind data on the TADI site was also collected using the TADI ZX 300 Wind Lidar measurement device, with measurement heights set to 10m, 20m, 38m, 50m, 75m, 100m, 125m, 150m, 180m, 240m, and 300m. Initially, it was not planned to share this wind data with the participating teams as each team had to use their own equipment as part of their technology deployment. However, to challenge the performers' results and especially their wind measurements, the TADI team decided to provide this information. Section S3.2 details the weather conditions. Flowrate information and detailed methane release schedules with location, start and end times, stabilization times, equipment numbers, and orientation can be found in Sect. S1.2.3.

### S3.2 Weather Conditions

Tables S11, S12, and S13 contain the weather, temperature, and wind conditions for each morning and afternoon during the campaign as recorded by the TADI site engineer using a 2d METEK meteorological station. More precise measurements of wind speed and direction were taken using the wind lidar measurement device.

**Table S11.** Daily weather conditions.

| **Week** | **Time of Day** | **Daily Weather Condition Recordings** | | | | |
|---|---|---|---|---|---|---|
| | | *Monday* | *Tuesday* | *Wednesday* | *Thursday* | *Friday* |
| **1** | *Morning* | Sunny, no clouds | Partly cloudy | Cloudy, wet, | Very rainy | Very cloudy with some rain |
| | *Afternoon* | Sunny, no clouds | Partly cloudy | Cloudy, without rain | Rainy | Very cloudy |

| | | | | | | |
|---|---|---|---|---|---|---|
| | | | | | | with some rain |
| **2** | *Morning* | Sunny, some clouds | Sunny | Cloudy | Cloudy | Cloudy |
| | *Afternoon* | Sunny, no clouds | Sunny | Cloudy | Cloudy | Cloudy |
| **3** | *Morning* | Continuous rain | Cloudy, some sun | Cloudy | Rainy | Cloudy |
| | *Afternoon* | Non-continuous rain | Sunny, some clouds | Drizzle | Cloudy, some showers, sunny late afternoon | Sunny, some clouds |
| **4** | *Morning* | Sunny, some clouds | Mist | Slightly cloudy | Partly cloudy | Partly cloudy |
| | *Afternoon* | Sunny, several clouds | Cloudy | Sunny, some clouds | Sunny, some clouds | Some clouds, rain showers |

**Table S12.** Daily temperature conditions.

| **Week** | **Time of Day** | **Daily Temperature Recordings (°C)** | | | | |
|---|---|---|---|---|---|---|
| | | *Monday* | *Tuesday* | *Wednesday* | *Thursday* | *Friday* |
| **1** | *Morning* | 30 | 22-24 | 18-22 | 15-16 | 18-19 |
| | *Afternoon* | 32-35 | 31-32 | 23-25 | 15-16 | 18-20 |
| **2** | *Morning* | 23-25 | 26-28 | 26-28 | 22 | 20-22 |
| | *Afternoon* | 27-30 | 32-34 | 38 | 30 | 30 |
| **3** | *Morning* | 16 | 16 | 17 | 13 | 11-12 |
| | *Afternoon* | 18-19 | 21-23 | 19 | 20-22 | 20-22 |
| **4** | *Morning* | 9-10 | 11-12 | 11-12 | 14 | 16-17 |

| | | | | | | |
|---|---|---|---|---|---|---|
| | *Afternoon* | 21-22 | 22-23 | 25-26 | 23-25 | 18-19 |

**Table S13.** Daily wind conditions.

| **Week** | **Time of Day** | **Daily Wind Conditions (m/s, direction)** | | | | |
|---|---|---|---|---|---|---|
| | | *Monday* | *Tuesday* | *Wednesday* | *Thursday* | *Friday* |
| **1** | *Morning* | 3-3.5 ESE | 1.4-2.6 SW | 1-3, W/WSW | No speed measuring, SSE | 3.5-5.5 W/WSW |
| | *Afternoon* | 1.5-3.7, E/ESE | 2-3.5, E/ENE | 3-4 WSW | 2-2.5 E/SE | 3.5-5.5 W/WSW |
| **2** | *Morning* | 2-3.5 N | 2-3.0 S/SSE/E | 1-3 E | 3-4 W/WNW | 1.5-2.0 W/WNW |
| | *Afternoon* | 2.5-3.0 E | 4.5-5 E | 2.5-3.5 E | 3-4 W/WNW | N/A |
| **3** | *Morning* | 3.5-5 W | 0.5-1 SW, later 1.5-3 | 3-4 SW, later 3.5-5 SW | 1-2 SW | 1-2 SW |
| | *Afternoon* | 2-3 W | 1.5-2 NE, later 2.5-3.5 SW | 3-4 SW | 3-4 SW | 3-4 SW |
| **4** | *Morning* | 1-2 SW | 1-2 SW | 1-2 ESE | 1-2 ENE | 1-2 SSE |
| | *Afternoon* | 2-4 SW | 1-2 SW | 1-2 E | 2-3 E | 1-2 SW |

In addition to the daily record of wind conditions, high-resolution wind data was collected using the ZX 300 Wind Lidar and released to all teams as part of the unblinding process. Figure S8 contains example releases with relatively better and worse wind conditions. In general, steady wind directions and moderate, steady wind speeds are preferred for most techniques, as they allow for more straightforward analysis. Very low winds and frequently changing wind directions tend to be difficult for most, if not all, analyzed techniques. Because of the natural experimental design (e.g., at a field site rather than in a controlled wind tunnel), we had no control over variation in wind quality across weeks.

## S3.3 Wind Rose Plots

Wind data are plotted in a wind rose plot, which provides information on wind speed and wind direction during the time of a specific release. Wind rose plots for each release over the four weeks of testing can be found below. Overall, wind conditions varied widely throughout each week and between each week of testing. Week 4 was particularly difficult, with average wind speeds that were very low and large variation of wind direction.

*Optimal wind conditions during Week 1*

*Difficult wind conditions during Week 4*

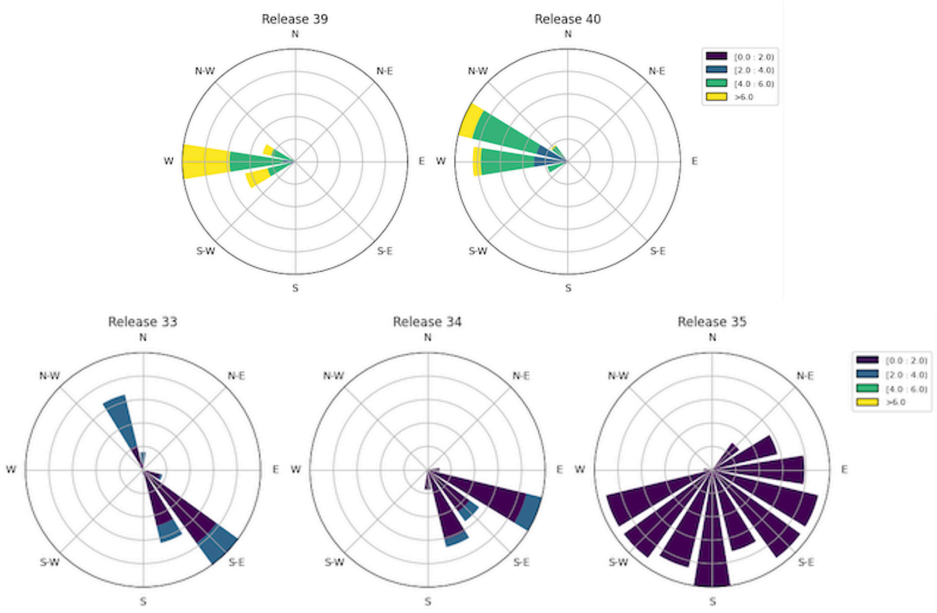



**Figure S8.** Wind rose plots characterizing the wind conditions during specific releases in Week 1 and 4. Low wind speeds and high variance of direction correspond to difficult conditions, while steadier winds with higher speeds and consistent direction are more optimal for measurement.

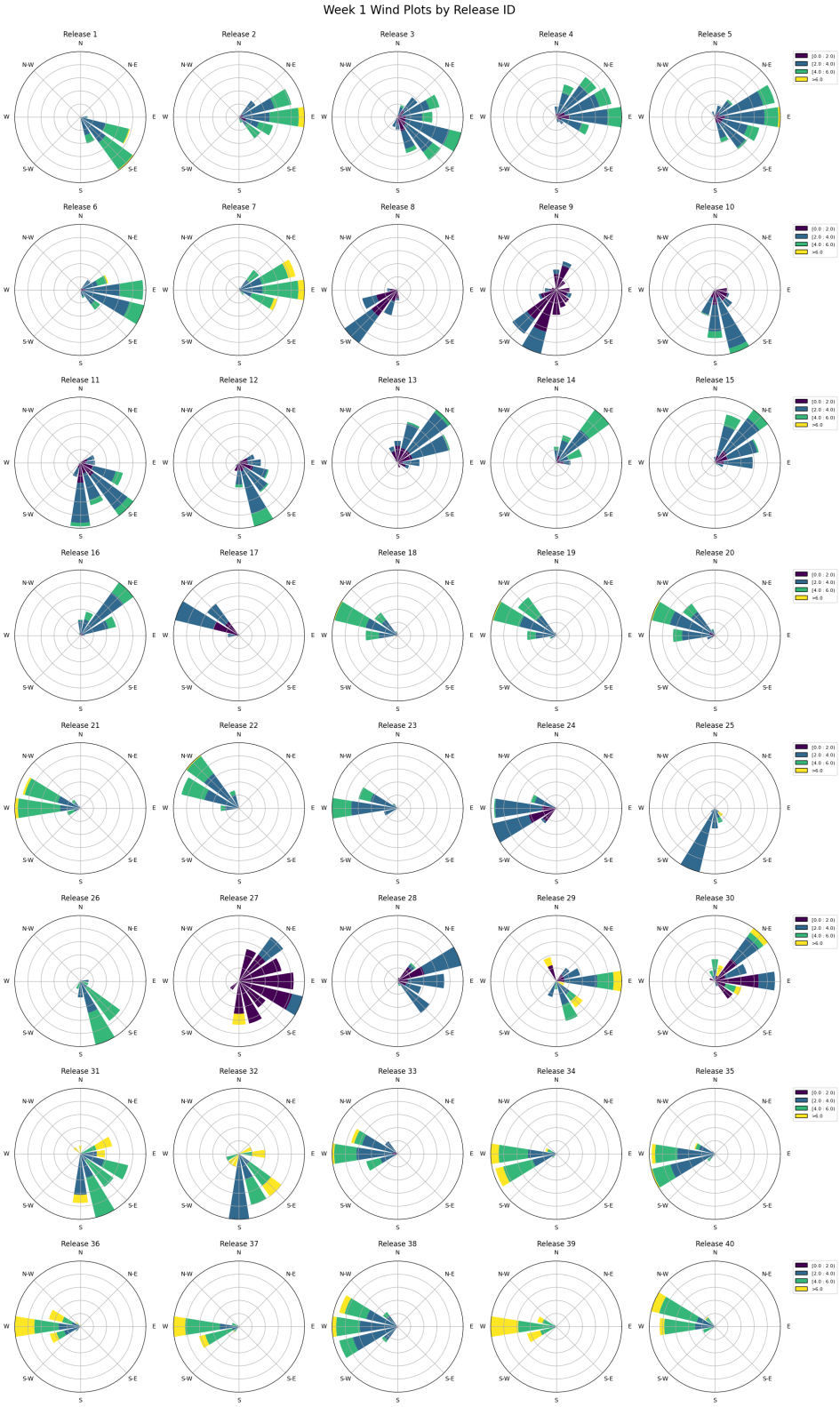



**Figure S9.** Week 1 wind rose plots by release.

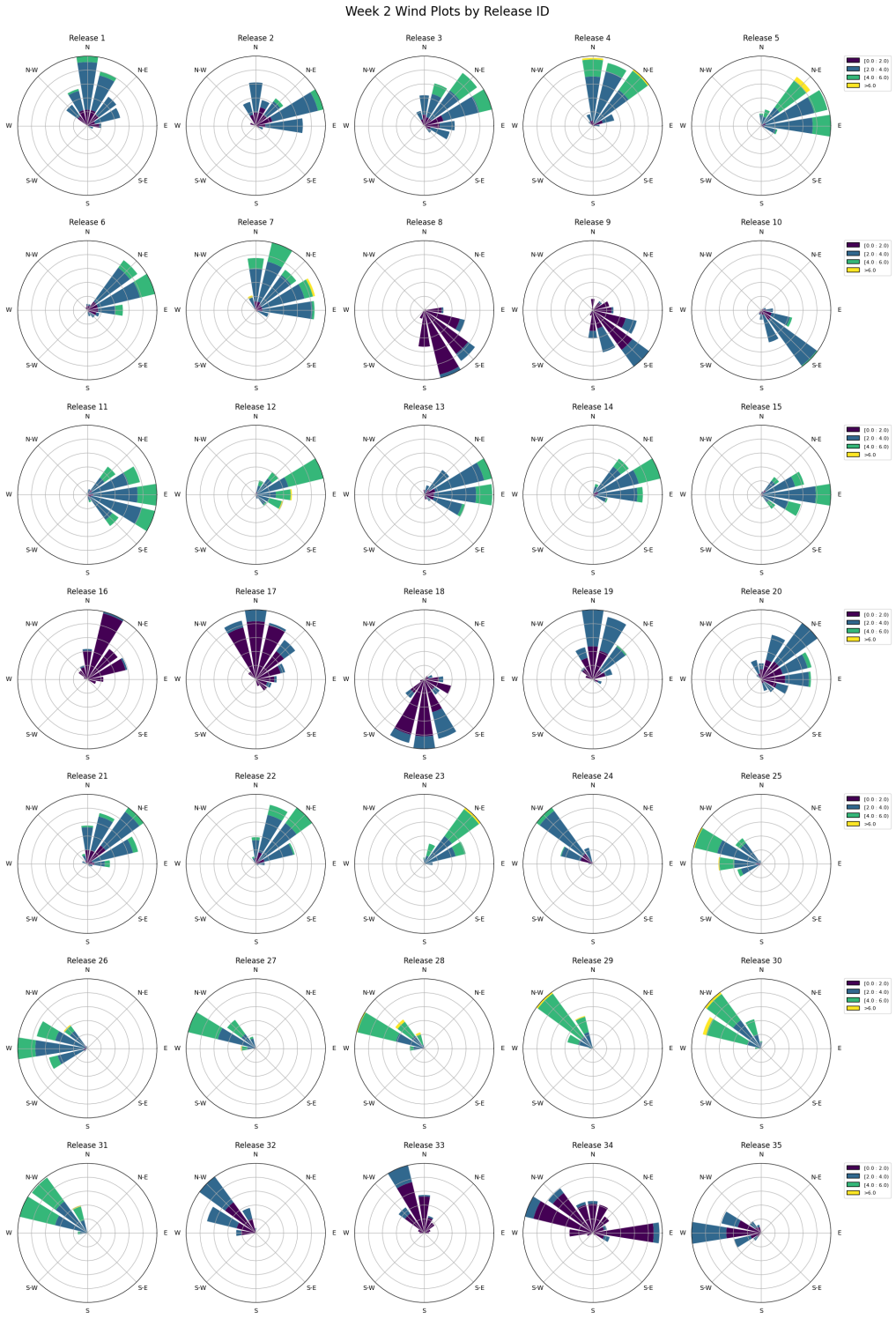



**Figure S10.** Week 2 wind rose plots by release.

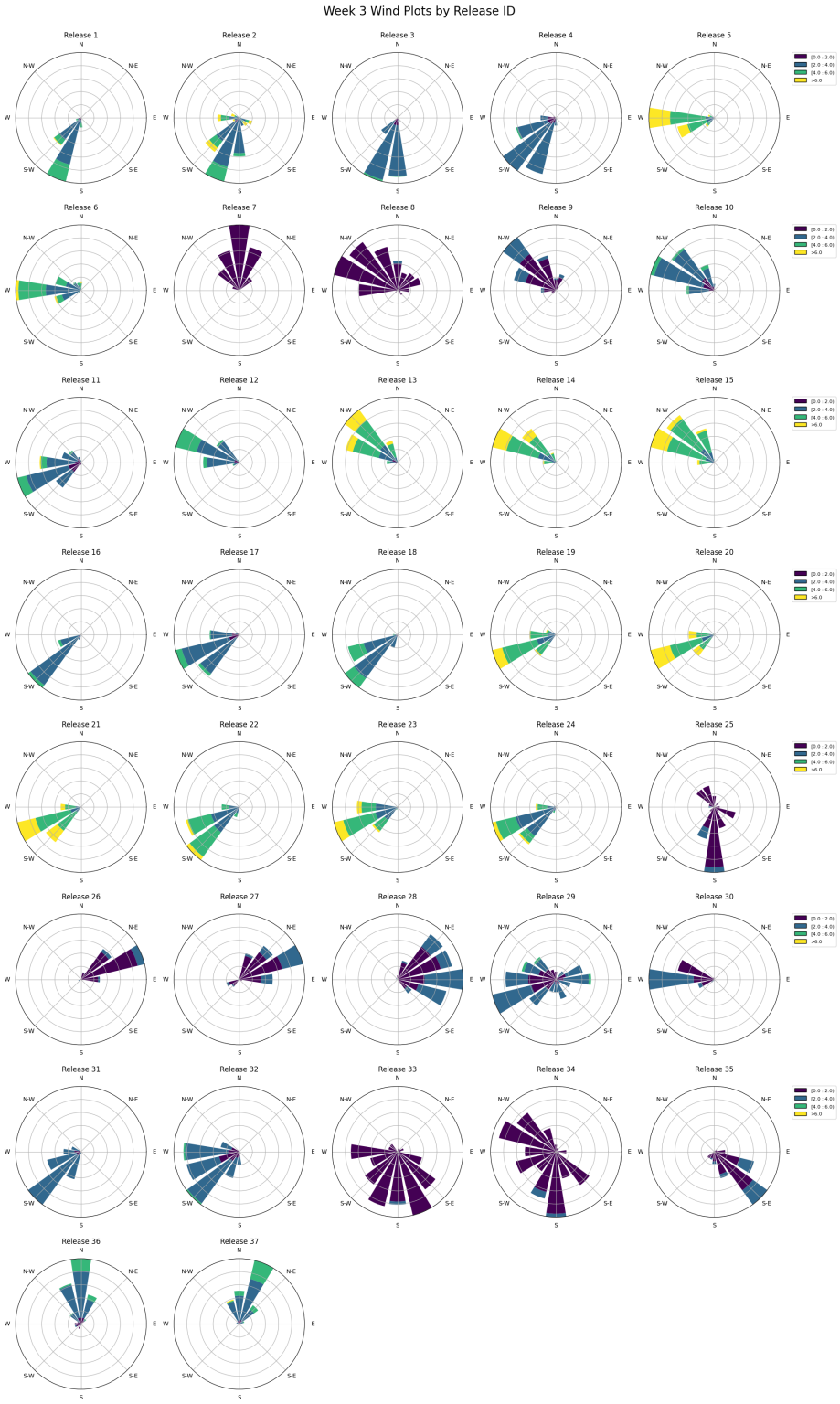



**Figure S11.** Week 3 wind rose plots by release.




**Figure S12.** Week 4 wind rose plots by release.

## S4 Participant Data Collection, Reporting, and Filtering

Throughout their week(s) participating in the campaign, the participants measured the methane releases to provide an estimate of the release flowrate. Each participant's measurement technique is described in Sect. S2.1, and in more detail submitted by participants in Sect. S2.3. Participants were allowed four weeks from the completion of each testing week to submit results for that week. Not all teams were able to perform analysis within four weeks, and we allowed additional time to reply given the provision that we would record the timing of response. We provided a Data Reporting Template to each participant with instructions on how to submit results. Table S14 contains the result submission dates of each participant.

**Table S14.** Results reporting dates and submission dates by participant and week.

| Week | Due Date | Team | Result Submission Date |
|---|---|---|---|
| 1 | July 22, 2024 | DTU | September 12, 2024 |
| 2 | July 29, 2024 | UHEI | August 9, 2024 |
| 3 | October 14, 2024 | FAAM | October 16, 2024 |
| 4 | October 21, 2024 | UU/LSCE/CYI/RHUL | December 2, 2024 |
| | | Empa/UZH | November 29, 2024 |

The Data Reporting Template also included sections for each participant to fill out with more detailed information on their technology, measurement techniques, and analysis methods. There were separate templates for each technology group: drone, vehicle, continuous monitor (fixed ground sensor), and aircraft/satellite. Additionally, each participant was sent the schedule ("Release Schedule") of the releases with start and end times and asked to fill out two columns verifying if they (1) measured the release ("Measurement Taken") and (2) were able to quantify the emission rate ("Quantification Status"). This information was then used to classify the releases, discussed in more detail in Sect. S4.1. Additionally, each team had the opportunity to point out if there were any specific issues with the quantification or detection of each release, such as wind or weather conditions or equipment malfunction. Each team was invited to submit as much additional information as they desired to, such as plume images, concentration paths, or any other context-providing document.

### S4.1 Participant Submission & Data Cleaning

Participants were asked to submit two documents: (1) the data reporting template with release rate estimates ("Results") and (2) a schedule of releases with information about whether participants had measured a particular release ("Schedule"). Although instructions were given on how to fill out these documents, each participant had a slightly different interpretation, leading to differences in how each team submitted release estimates. The Stanford team developed three different criteria to filter and categorize each participants results: a strict data filtering criterion (Strict QC), the Stanford team's criteria (Stanford QC), and a participant-submitted criteria (Participant QC). Results estimates were categorized into one of three types of estimates: releases that teams measured and submitted a non-zero methane emission rate ("non-zero estimates"), releases for which teams submitted a methane emission rate of 0 kg/h ("zero estimates"), and releases for which teams did not submit any estimate ("N/A estimates"). Participants submitted zero-estimates differently (e.g. some reported in an estimate methane emission rate of 0 kg/h, while others reported them as failed quantifications), resulting in the creation of the three different categorization methods (Strict QC, Stanford QC, and Participant QC). Unless otherwise specified, the Stanford QC process was the default method used for data included in analysis.

#### S4.1.1 Data filtering and categorization methods

The three different QC methods used the information that teams submitted in the Schedule document to categorize a release estimate into non-zero, zero, or N/A. This used the information in the three columns in the Schedule: (1) Measurement Taken, (2) Quantification Status, and (3) Explanation. The difference in each method is in how they treat releases that were submitted as failed quantifications. The Strict QC criteria considered every release that was measured as passing QC, and assigned release rates of 0 kg/h to every release that did not have an associated estimate submitted. The Stanford QC criteria assigned either 0 kg/h or N/A to releases that were reported as failed quantifications, depending on the explanation that the participant provided. The Participant QC criteria only included release estimates that had an associate methane emission rate submitted by the participant. This information is summarized in Table S15.

**Table S15.** Participant release estimate filtering criteria

| **Release Schedule Column[a]** | | **QC Criteria** | | |
|---|---|---|---|---|
| *Measurement Taken* | *Quantification Status* | *Strict QC* | *Stanford QC* | *Participant QC* |
| YES | Completed | As reported | As reported | As reported |

| | | | | |
|---|---|---|---|---|
| YES | Failed | Zero | Depends on Explanation | N/A |
| NO | N/A | N/A | N/A | N/A |

[a] The criteria use the information provided in the "Release Schedule" document. Participants were to turn in this document along with the Data Reporting Template that contained their estimated emission rates.

Participants occasionally did not report measurements for some releases they had measured due to quality issues with the measurements and subsequent analysis. Examples of data quality issues include low wind speeds, cloud coverage, and equipment malfunction. Additionally, some participants reported releases that were below their detection limits as failed quantifications, while others reported in release rates of 0 kg/h. The Stanford QC process aimed to address this difference in reporting. In general, failed quantifications with explanations related to detection capabilities or low signals were categorized as zero-estimates while other issues were categorized as N/A (Fig. S13). The participant-specific release estimate categorization for releases with entries in the Explanation column using the Stanford QC criteria is described in Sects. S4.1.2–S4.1.6, and flow rate charts for each specific participant are provided below. The QC flags included by each participant are also included in a table.

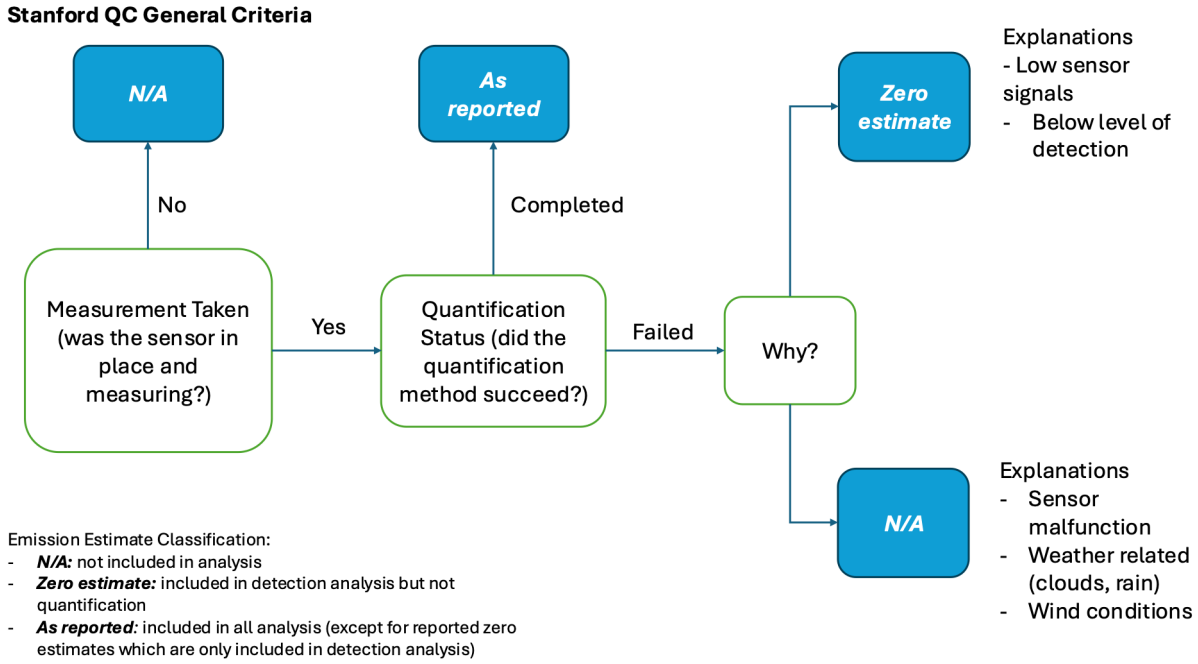



**Figure S13.** Stanford QC process release estimate classification criteria.

### S4.1.2 DTU Data Cleaning

DTU did not submit a schedule as requested; however, all the information is in the results spreadsheet, and they measured every release during their week. They submitted an estimate for

all releases except for ones they designated as below their level of detection. Table S16 contains DTU's QC flags and associated Emission Rate Classification.

**Table S16. DTU QC flags with number of releases and associated estimated emission rate.**

| QC Flag | Number of Releases | Stanford QC Assigned Emission Rate (kg/h) |
|---|---|---|
| Below detection limit | 3 | 0 |

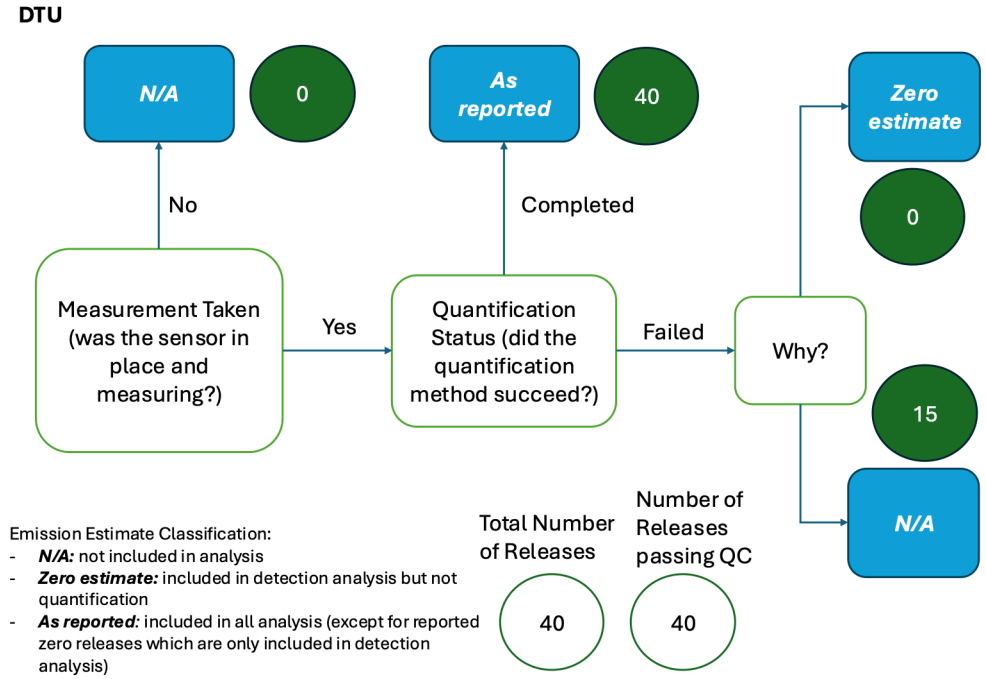



**Figure S14. Data cleaning process flowchart for DTU.**

### S4.1.3 UHEI Data Cleaning

The Heidelberg University team reported all releases in their Data Reporting results spreadsheet, including ones that they did not measure or failed to quantify. Calculated emission rates were reported with not valid flags when the wind speed was below 2 m/s. They additionally submitted concentration path maps for each estimate. Table S17 contains UHEI's QC flags and associated Emission Rate Classification.

**Table S17. UHEI QC flags with number of releases and associated estimated emission rate.**

| QC Flag | Number of Releases | Stanford QC Assigned Emission Rate (kg/h) |
|---|---|---|
| Car not available | 1 | N/A |
| Unfavorable wind conditions<br>ws < 2m/s, instable wd | 15 | N/A |

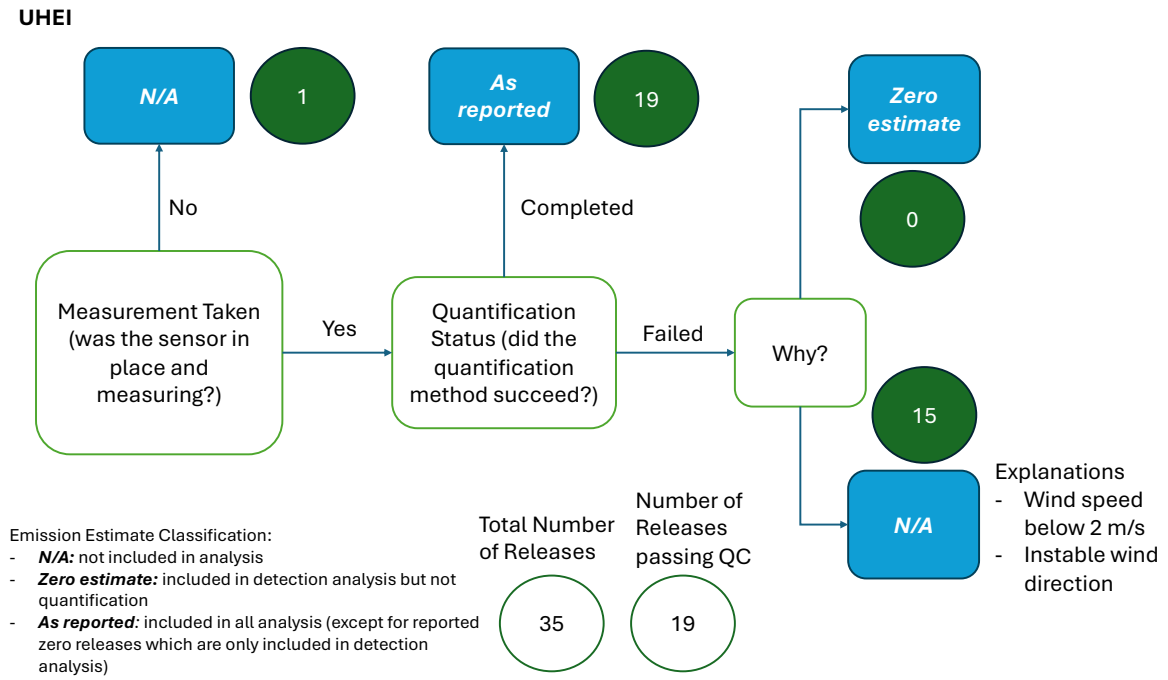



**Figure S15. Data cleaning process flowchart for UHEI.**

### S4.1.4 UU/LSCE/CYI/RHUL Data Cleaning

Originally, we were expecting results from three teams: CYI/LSCE, UU, and RHUL. After the completion of the testing period, these teams decided to separately analyze their results but submit an averaged estimate for their final combined result. The combined team merged only similar estimates into the reported values. If one sub-team had a significantly different estimate for one release, then this 'outlier' value was not merged into the official reporting. Table S18 contains this team's QC flags and associated Emission Rate Classification.

**Table S18. UU/LSCE/CYI/RHUL QC flags with number of releases and associated estimated emission rate.**

| QC Flag | Number of Releases | Stanford QC Assigned Emission Rate (kg/h) |
|---|---|---|
| Overlapped with other activity | 2 | N/A |
| Aeris malfunctioning and no wind conditions | 1 | N/A |
| Unable to identify source location | 1 | N/A |
| GPS data loss | 1 | N/A |
| Heavy rain. No good signal found. | 1 | N/A |

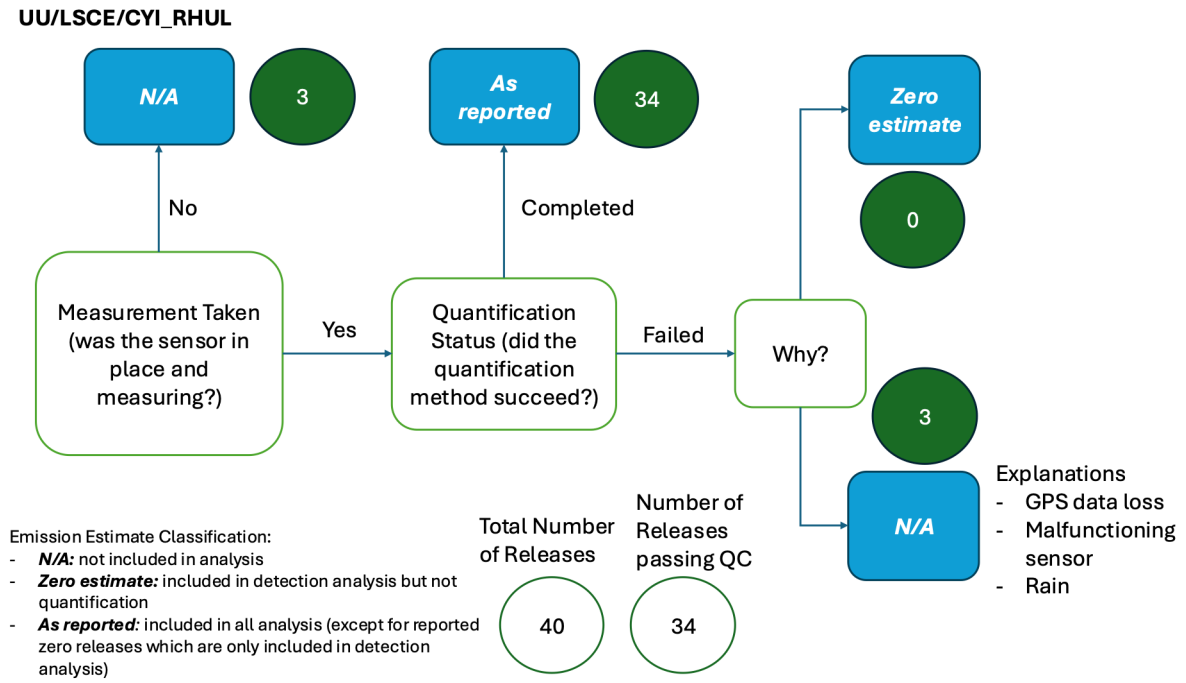



**Figure S16. Data cleaning process flowchart for UU/LSCE/CYI/RHUL.**

### S4.1.5 Empa/UZH Data Cleaning

During a single release, the Empa/UZH aircraft would record several overpasses over the site. They submitted the average of the overpasses with their results and that was used in the analysis. They also included individual overpass flowrate estimates. Table S19 contains their QC flags and associated Emission Rate Classification. Note that the releases with the flag "no plume visible" were treated as zeros for analysis (i.e. below the detection limit of the aircraft)

**Table S19. Empa/UZH QC flags with number of releases and associated estimated emission rate.**

| QC Flag | Number of Releases | Stanford QC Assigned Emission Rate (kg/h) |
|---|---|---|
| Bad weather (clouds, rain, fog) | 22 | N/A |
| No plume visible | 6 | 0 |
| Aircraft refueling | 2 | N/A |
| Cloud shadow over site => no plume detected | 1 | N/A |

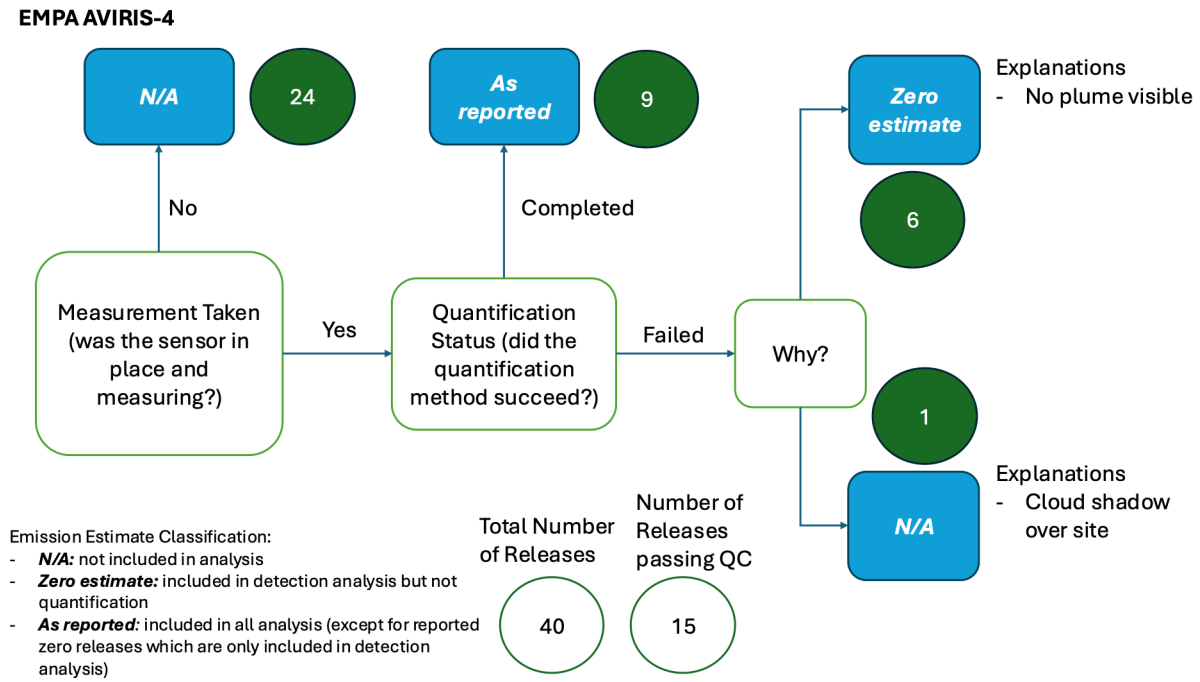



**Figure S17. Data cleaning process flowchart for Empa/UZH.**

### S4.1.6 FAAM Data Cleaning

Due to scheduling and budget constraints and airspace restrictions around the TADI site, FAAM was only able to participate in one day of releases (Thursday, September 12, 2024). Weather conditions made flying difficult in the morning, meaning they were only able to measure three releases, with two of those releases at a farther distance. Table S20 contains FAAM's QC flags and associated Emission Rate Classification.

**Table S20. FAAM QC flags with number of releases and associated estimated emission rate.**

| QC Flag | Number of Releases | Stanford QC Assigned Emission Rate (kg/h) |
|---|---|---|
| Not able to fly (transit flights or not in France) | 29 | N/A |
| Not able to fly due to low clouds | 4 | N/A |
| Late take off | 1 | N/A |
| Not enough time for data analysis | 2 | N/A |

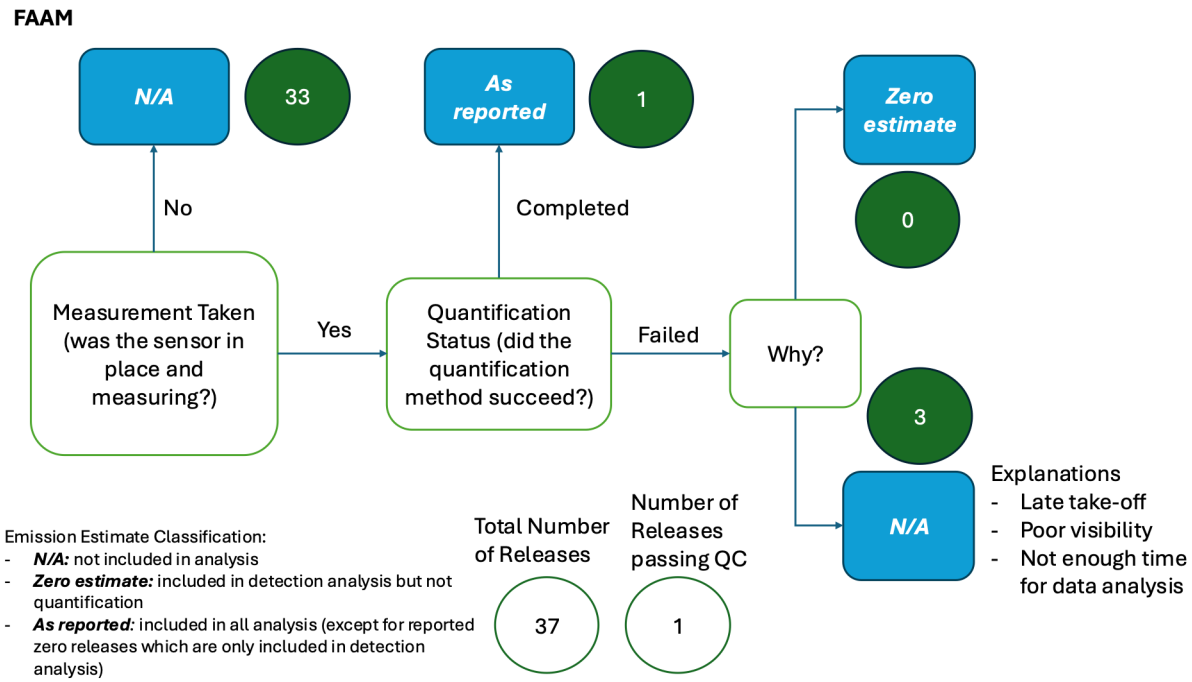



**Figure S18. Data cleaning process flowchart for FAAM.**

## S4.2 Data classification

Table S21 summarizes the release estimates that pass the data filtering and categorization process for each participant using each of the QC methods. Note that in many cases the Stanford QC and Participant QC processes result in the same number of zero and non-zero release estimates. Table S22 contains the minimum and maximum true release rates measured by each team. This does not mean that the team necessarily submitted an estimate for this true release rate, only that they were measuring during the release.

**Table S21. Release counts by participant through the filtering process.**

| Solution | Scheduled Releases | Measured Releases | Strict QC Passing Estimates | | | Stanford QC Passing Estimates | | | Participant QC Passing Estimates | | |
|---|---|---|---|---|---|---|---|---|---|---|---|
| | | | *Zero* | *Non-Zero* | *Total* | *Zero* | *Non-Zero* | *Total* | *Zero* | *Non-Zero* | *Total* |
| *DTU* | 40 | 40 | 3 | 37 | 40 | 3 | 37 | 40 | 3 | 37 | 40 |
| *UHEI* | 35 | 34 | 15 | 19 | 34 | 0 | 19 | 19 | 0 | 19 | 19 |
| *UU/LSCE/CYI/RHUL* | 40 | 37 | 4 | 33 | 37 | 1 | 33 | 34 | 1 | 33 | 34 |
| *Empa/UZH* | 40 | 16 | 7 | 9 | 16 | 6 | 9 | 15 | 0 | 9 | 9 |
| *FAAM* | 8 | 4 | 3 | 1 | 4 | 0 | 1 | 1 | 0 | 1 | 1 |

*Scheduled releases refer to the total number of releases available for each performer occurring during the assigned week(s) of testing. Measured releases is the number of releases that the participants measured during the testing periods. This is the same as the total number of releases passing the Strict QC criteria. QC passing estimates is the number of measured estimates that passed the three QC methods, divided into zero and non-zero estimates by participant (i.e. the classification of the release rate submitted by the participant, which could be different than the true release rate). The Stanford QC passing releases are those included in the analysis in the Results section (highlighted in gray).*

**Table S22. Maximum and minimum true release rates measured and passing the QC process.**

| Solution | Maximum Release Rate Measured [kg/h] | Minimum Release Rate Measured [kg/h] | Maximum Release Rate Passing Stanford QC [kg/h] | Minimum Release Rate Passing Stanford QC [kg/h] |
|---|---|---|---|---|
| *DTU* | 126.0 | 0.0 | 136.0 | 0.0 |
| *UHEI* | 189.9 | 0.0 | 136.0 | 0.0 |
| *UU/LSCE/CYI/RHUL* | 290.0 | 0.0 | 290.0 | 0.0 |
| *Empa/UZH* | 290.0 | 0.0 | 290.0 | 0.29 |
| *FAAM* | 210.0 | 1.3 | 210.0 | 210.0 |

**These are the true release rates corresponding to estimates that (1) the participant measured and (2) pass the Stanford QC process. The release schedules were planned so each participant would measure during a satellite-scale and zero-release, but due to equipment and weather issues this was not possible for every participant.**

## S4.3 Solution Uncertainties

Table S23 contains the confidence level associated with the upper and lower emission rate estimates submitted with participants' results, as well as the sources of uncertainty that they include in their quantification estimates.

**Table S23. Uncertainty types associated with participant quantification of release flowrates.**

| Solution | Confidence Level | Uncertainty Source |
|---|---|---|
| *DTU* | 95% CI, SEM | Standard error of the mean. |
| *UHEI* | SEM | Standard error of the median |
| *UU/LSCE/CYI/RHUL* | N/A | Each sub-team (UU, CYI/LSCE, RHUL) evaluated their own uncertainty over their own results. They evaluated the uncertainty based on the variance across all individual emission estimates from all (QC-approved) peaks for each release. This provided the uncertainty assessment for each sub-team estimate of the release. For reporting purposes, they propagated the uncertainty of individual results to the final team-official reported value. |
| *Empa/UZH* | 1-sigma | The uncertainty of the estimated emissions is obtained by performing error propagation of the individual sources of uncertainty. |

| | | |
|---|---|---|
| *FAAM* | 1-sigma | Uncertainty expressed as statistical spread around mean |

**Note that SEM refers to Standard Error of the Mean. See Participant Technology Survey Reponses in Sect. S2.3 for more detailed responses on uncertainty.**

## S5 Detection Results

### S5.1 Release Classification Criteria

The ability of methane detection technologies to correctly identify the presence of emissions is a fundamental requirement for effective emissions monitoring and mitigation. In this section, we evaluate the detection performance of each participant by categorizing reported measurements as true positives (TP), false positives (FP), true negatives (TN), or false negatives (FN). True positives indicate successful detection of a known release, while false negatives represent missed detections. Conversely, false positives occur when a participant reports a detection where no release was present, and true negatives confirm correct identification of zero-release events. The general criteria for these designations can be found in Table S24.

**Table S24.** General release categorization criteria into TP, TN, FP, and FN.

| Categorization | True Release Rate | Participant Estimated Release Rate[a] |
|---|---|---|
| TP | >0 | >0 |
| TN | 0 | 0 |
| FP | 0 | >0 |
| FN | >0 | 0 |

[a] The participant release rate refers to the reported release rate or release rate assigned during the data categorization process.

### S5.2 Detection Capabilities Under 5 kg/h

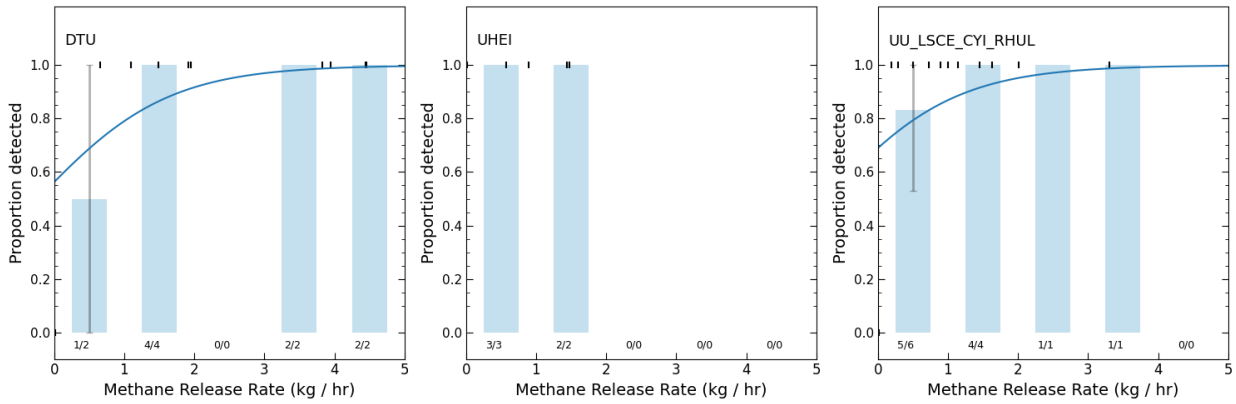



**Figure S19.** Detection capabilities below 5 kg $h^{-1}$.

This figure shows the probability of detection for participant-quantified releases. Each release is marked by a vertical line at y = 0 if not detected and y = 1 if detected, ordered along the x-axis by release volume. Blue bars indicate the proportion of detected releases within each bin, with error bars representing 95% confidence intervals based on a binomial distribution. The darker blue line is the best fit of a logistic regression model on the probability data. Empa/UZH and FAAM are excluded due to not measuring any releases below 5 kg $CH_4$ $h^{-1}$. The x-axis is based on the true release rate.

## S5.3 Distribution of Detected Releases

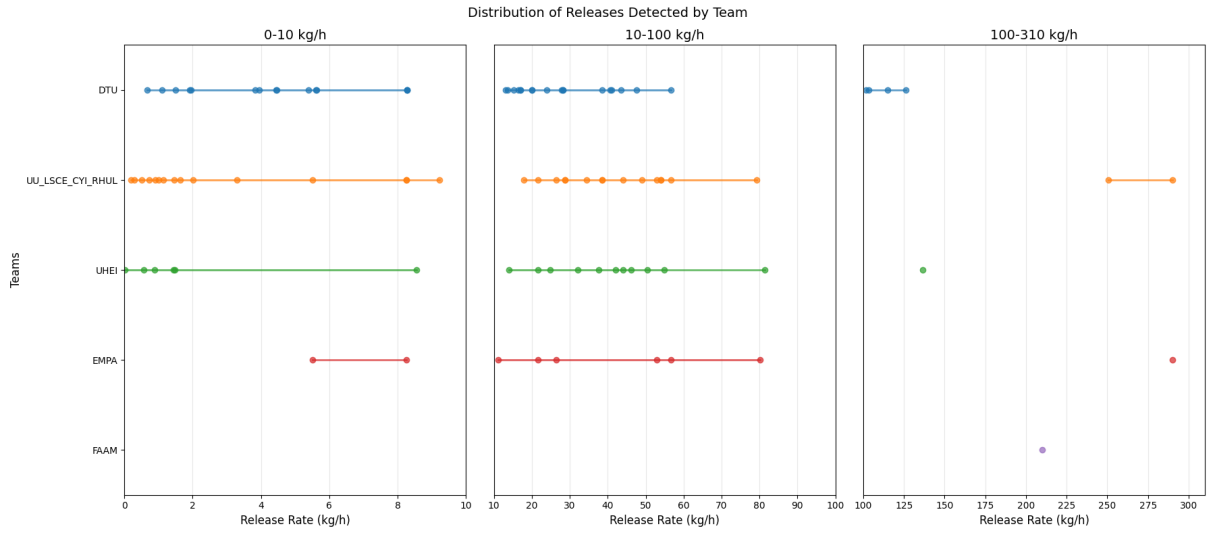



**Figure S20.** Distribution of detected releases by participant.

## S5.4 UHEI non-zero release detection

The UHEI team claims that something may have gone wrong during one of the zero-release experiments. While circling the facility, they state they clearly observed elevated $CH_4$ concentrations downwind of the site—between 90 and 950 ppb higher than background levels. They presented this finding during post-unblinding analysis. The other teams that measured during this release did not report any unusual findings, so this is included as a false positive in the analysis.

## S6 Quantification Results

## S6.1 Parity Plots for Releases Below 100 kg $h^{-1}$ and Above 10 kg $h^{-1}$

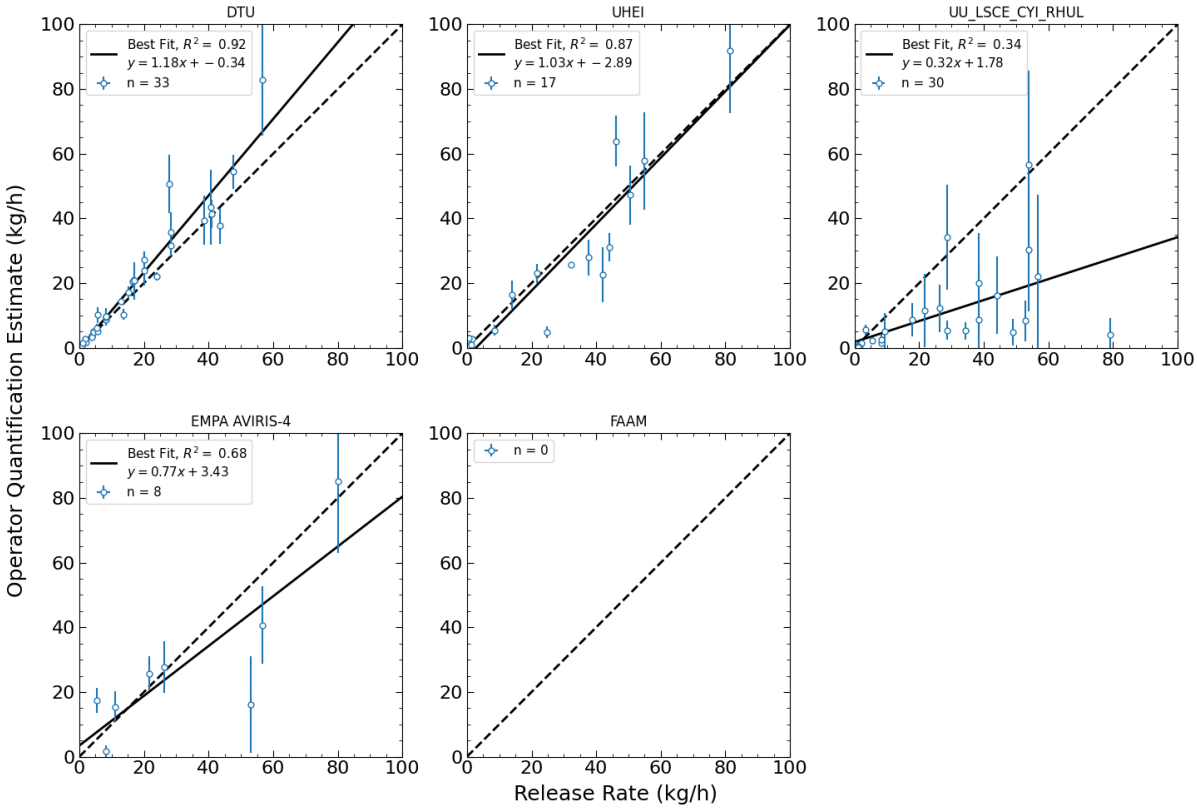



**Figure S21.** Parity plots with true release rates of <100 kg $h^{-1}$

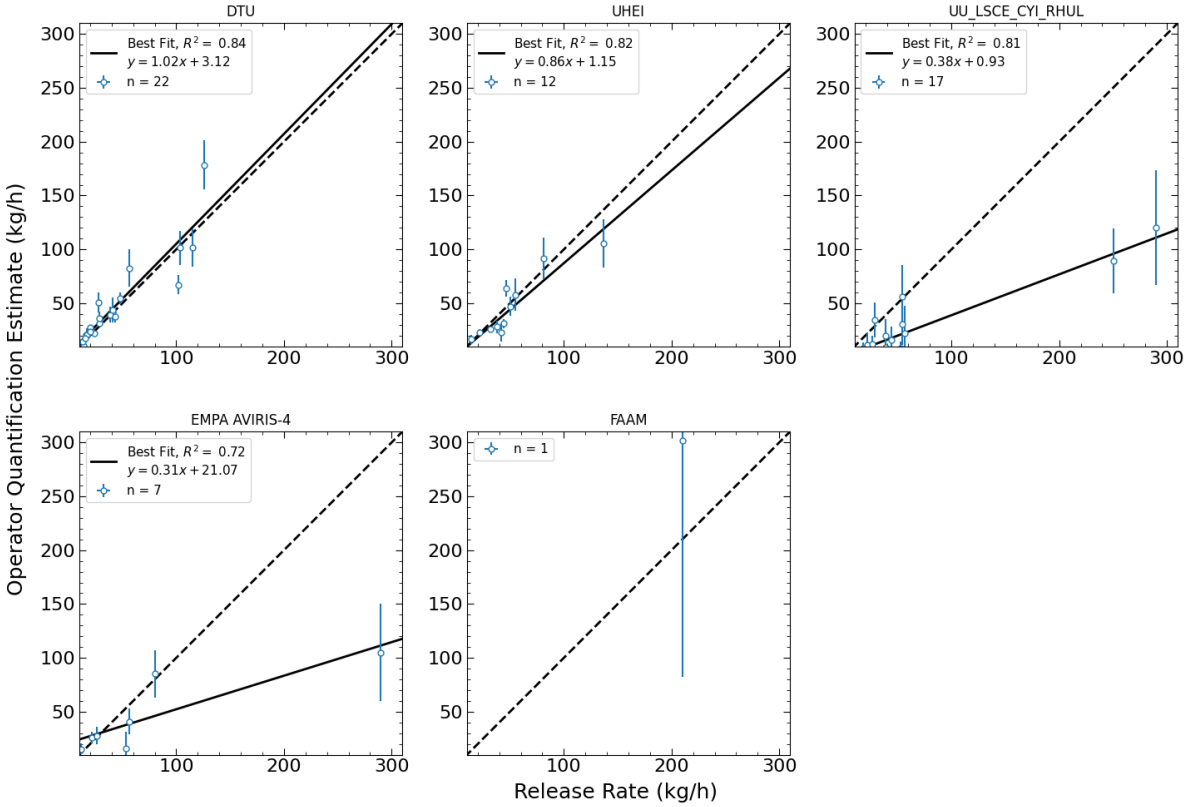



**Figure S22.** Parity plots with true release rates > 10 kg $h^{-1}$

## S6.2 Participant Parity Plots

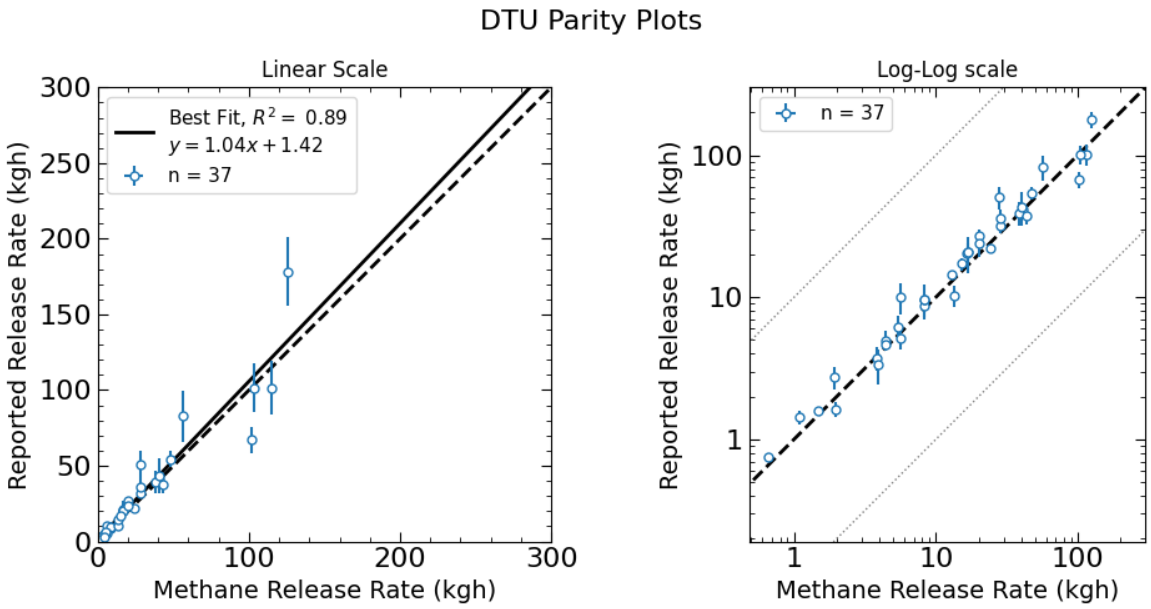


**Figure S23. DTU parity plot.**

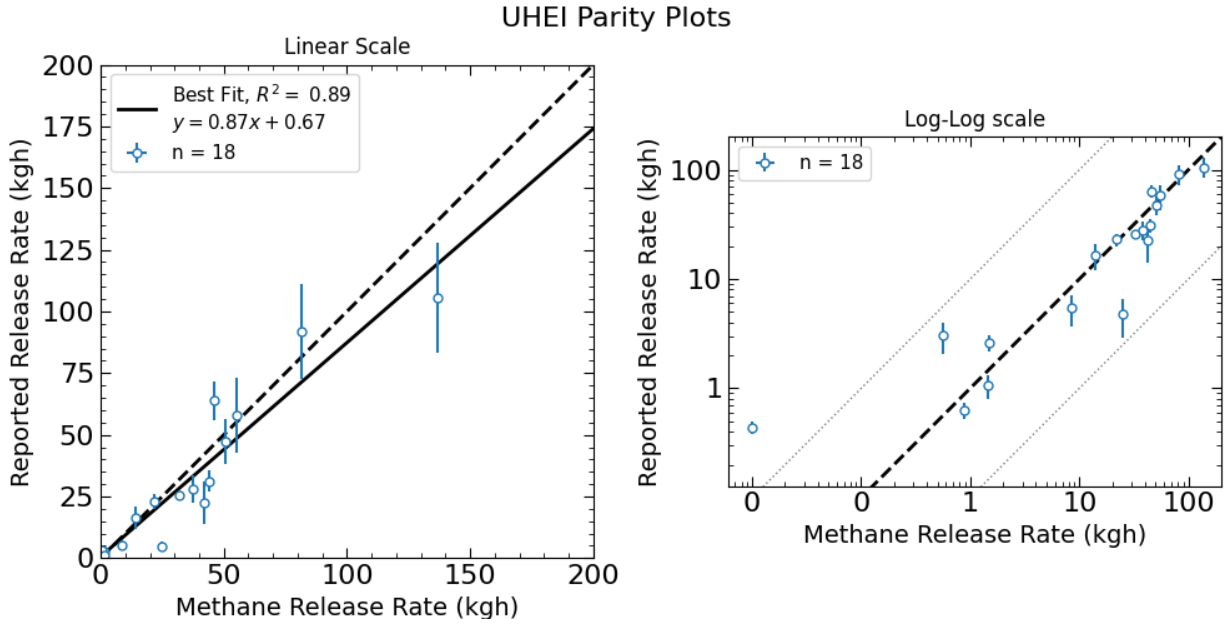



**Figure S24. UHEI parity plot.**

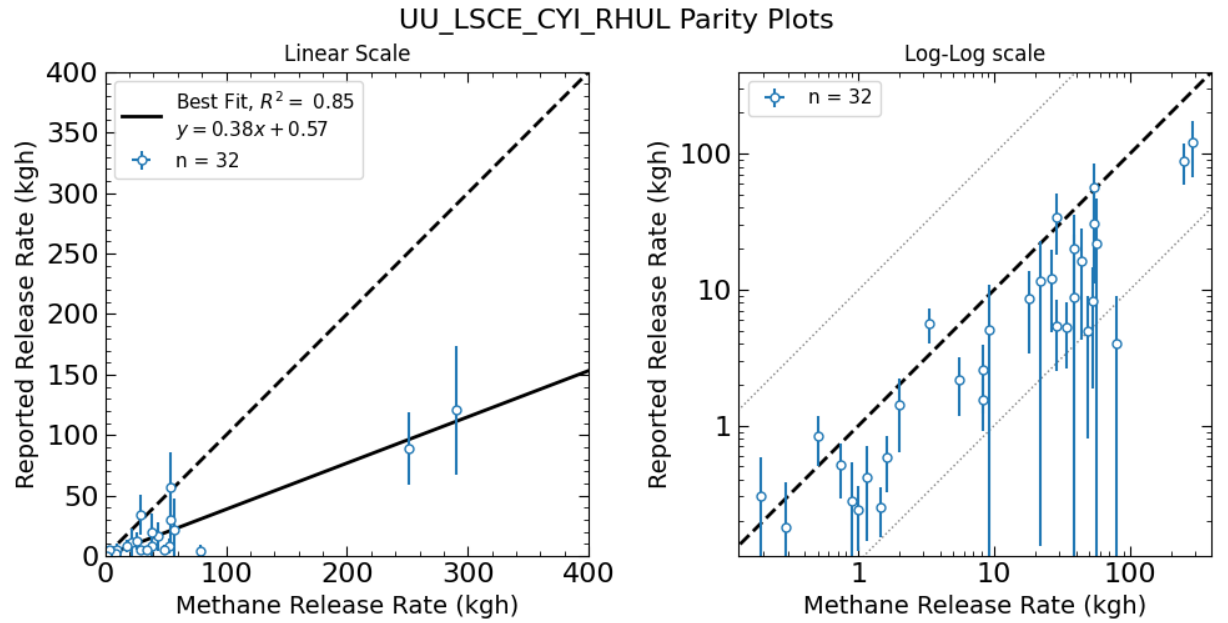



**Figure S25. UU/LSCE/CYI/RHUL parity plot.**

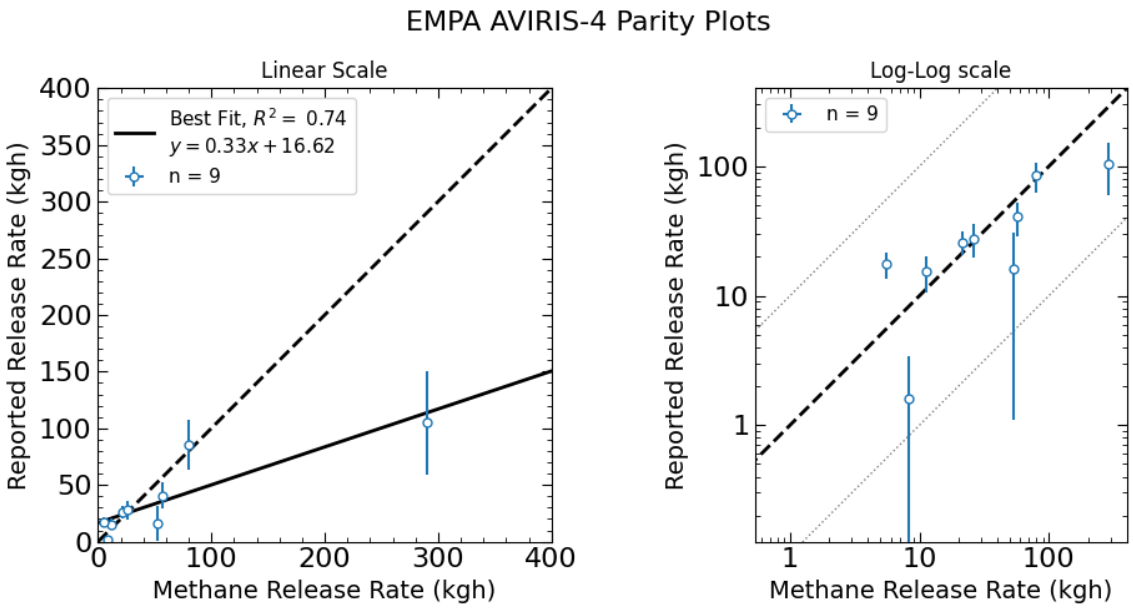



**Figure S26. Empa/UZH parity plot.**

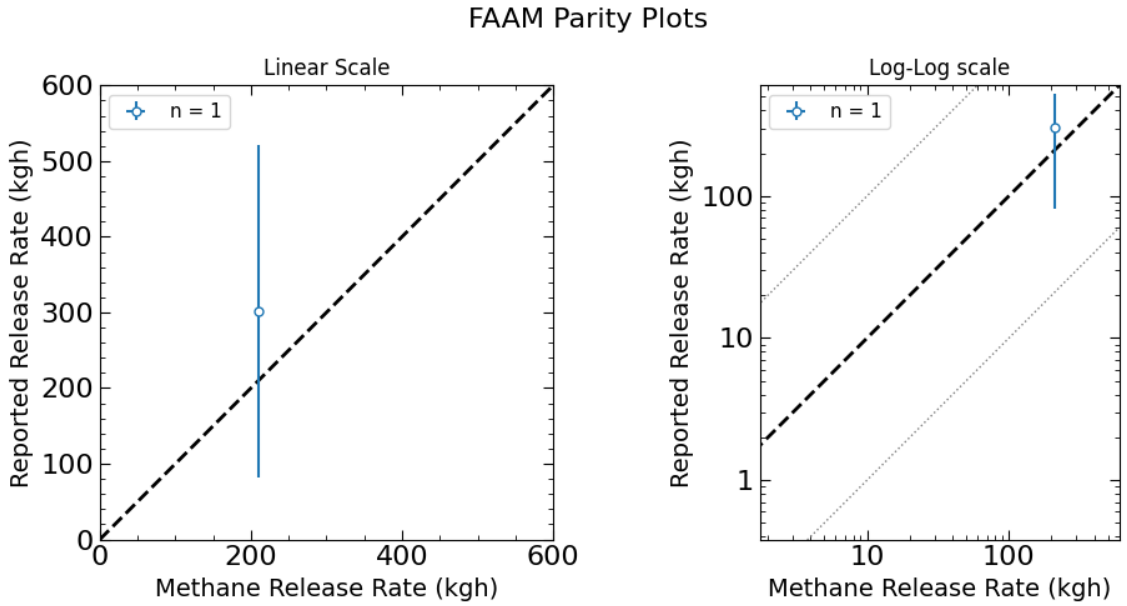



**Figure S27. FAAM parity plot.**

## S6.3 Uncertainty-weighted Regression of Quantification Estimates

All parity regressions reported in the main text use ordinary least squares (OLS). Because every academic team also submitted an uncertainty estimate alongside each quantified emission rate, we repeated these regressions using uncertainty-weighted least squares as a sensitivity analysis.

The metered release rate is known to within the accuracy of the TADI metering system and no per-release uncertainty was propagated for it, so the general errors-in-variables problem reduces to weighting only the operator-reported estimate; we therefore fit a weighted least-squares model with weights $w_i = \frac{1}{\sigma_i^2}$. Teams described their reported bounds using different conventions (95 % confidence intervals, ±1 standard deviation, 3σ, and the standard error of the mean or median), so the submitted bounds were first normalised to a common 1σ scale by dividing each reported half-width by its declared coverage factor. Reported intervals were asymmetric for 6 of the 97 quantified releases, and for these the two half-widths were averaged. All five academic teams reported uncertainties for every release entering the parity analysis, so no values were imputed; FAAM quantified only one release and is therefore excluded from both fits. Results are plotted in Fig. S28.

Weighting changes the fitted slopes materially and in both directions: DTU is essentially unchanged (1.04 → 1.07), UHEI decreases modestly (0.87 → 0.79), UU/LSCE/CYI/RHUL becomes substantially shallower (0.38 → 0.17), and EMPA/UZH becomes steeper (0.34 → 0.61). We note that the conclusions drawn in the main text — that quantification accuracy varies widely between teams and that no team achieves parity across the full range of release rates — are unchanged under either estimator.

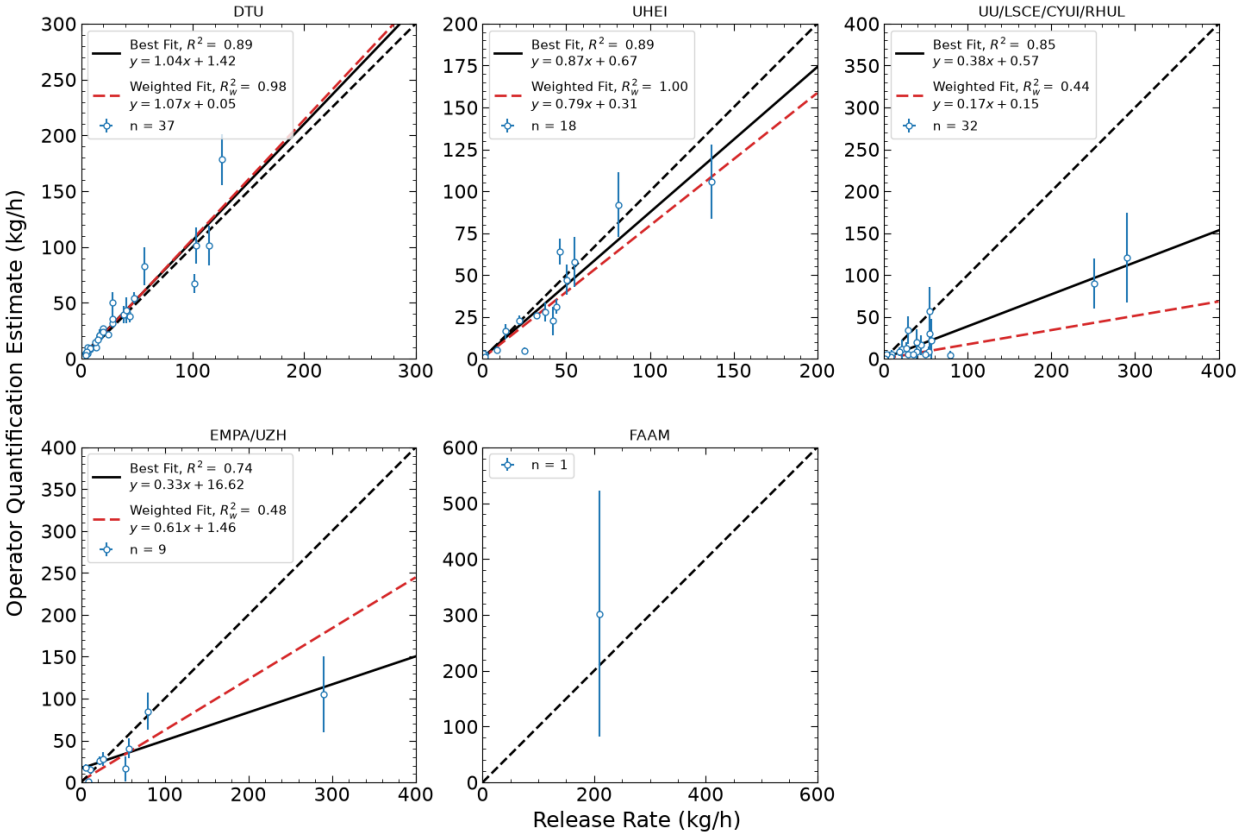



**Figure S28. Parity plots for the academic teams showing the unweighted (OLS, solid black) and uncertainty-weighted (WLS, dashed red) linear fits.**

**Error bars are the operator-reported uncertainties as submitted; the dashed 1:1 line indicates parity. FAAM quantified a single release, so no fit is shown.**

## S7 Wind Condition Analysis

Wind conditions significantly influence methane plume behavior, affecting detection and quantification accuracy. Variability in wind speed, direction, and turbulence can distort plume shape and movement, making accurate measurement more challenging—especially under rapidly changing conditions. This section analyzes measurement performance across bins of average wind speed, wind speed CoV, and wind direction CoV to identify where different technologies perform best or face limitations. Results are shown both by participant and in aggregate, though data point counts vary across participants.

Wind data were collected using TADI's ZX 300 Wind Lidar at 20 m height and were not available to participants until after unblinding. Wind statistics were calculated for each release window. Coefficient of variation (CoV), defined as the standard deviation normalized by the mean, was used to assess variability. Figures S29–S31 show parity plots colored by wind speed and variability bins.

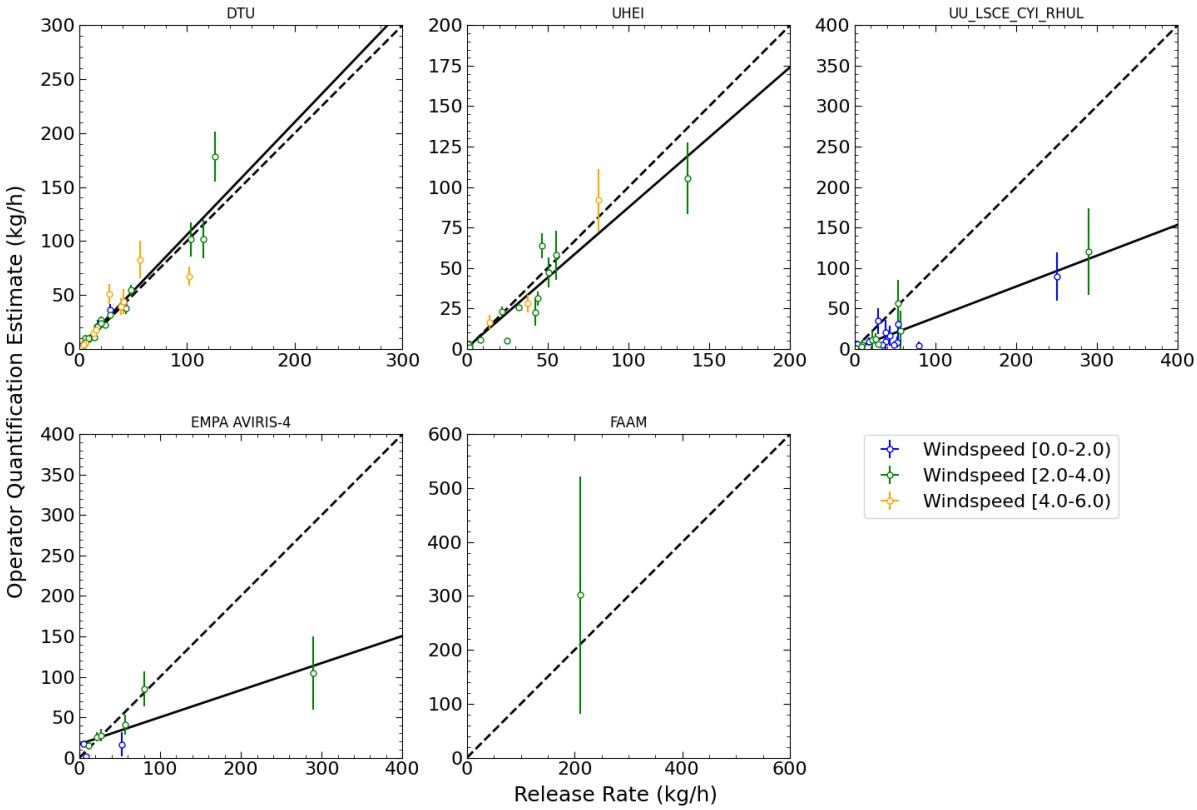



**Figure S29.** Parity plots with average wind speeds.
The average windspeeds are binned into low [0-2.0 m/s), medium [2-4 m/s) and high [4-6 m/s) windspeed bins.

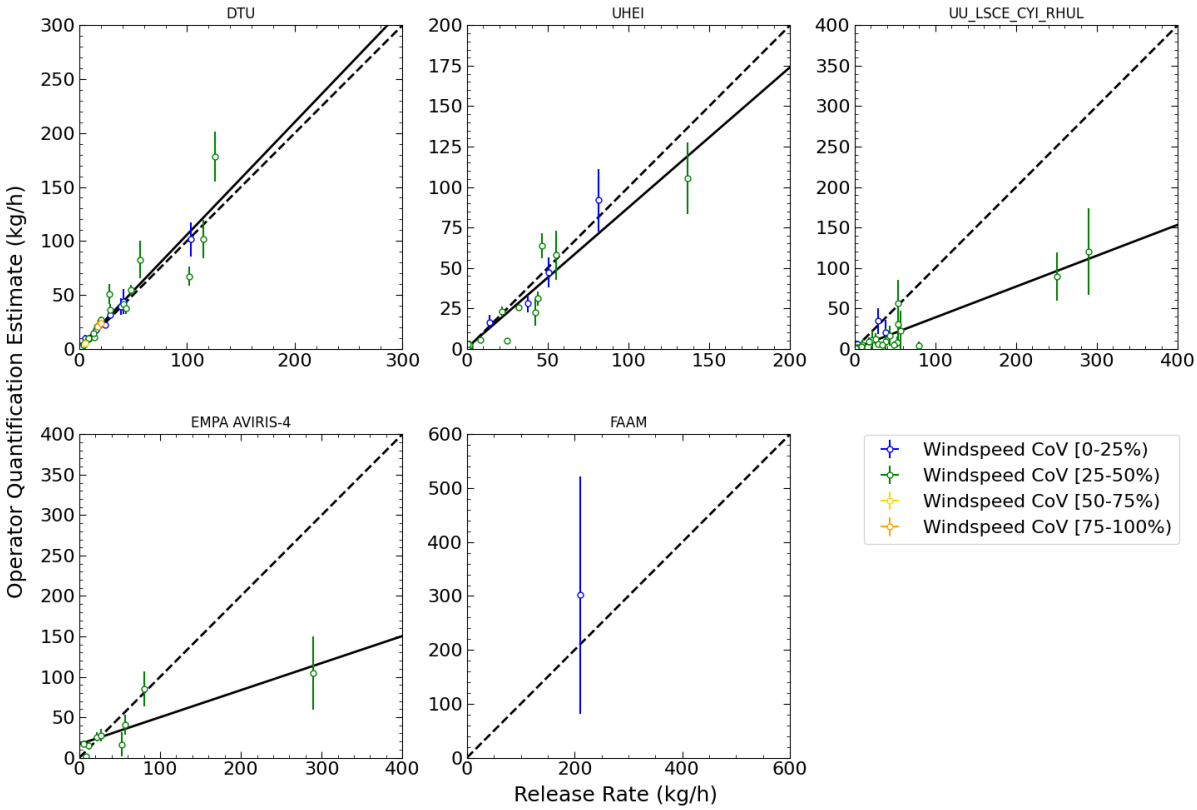



**Figure S30.** Parity plots with wind speed coefficient of variation (CoV).
The average wind speed CoVs are binned into low [0-25%), medium [25-50%), high [50-75%), and extreme [75-100%) wind speed CoV ranges.

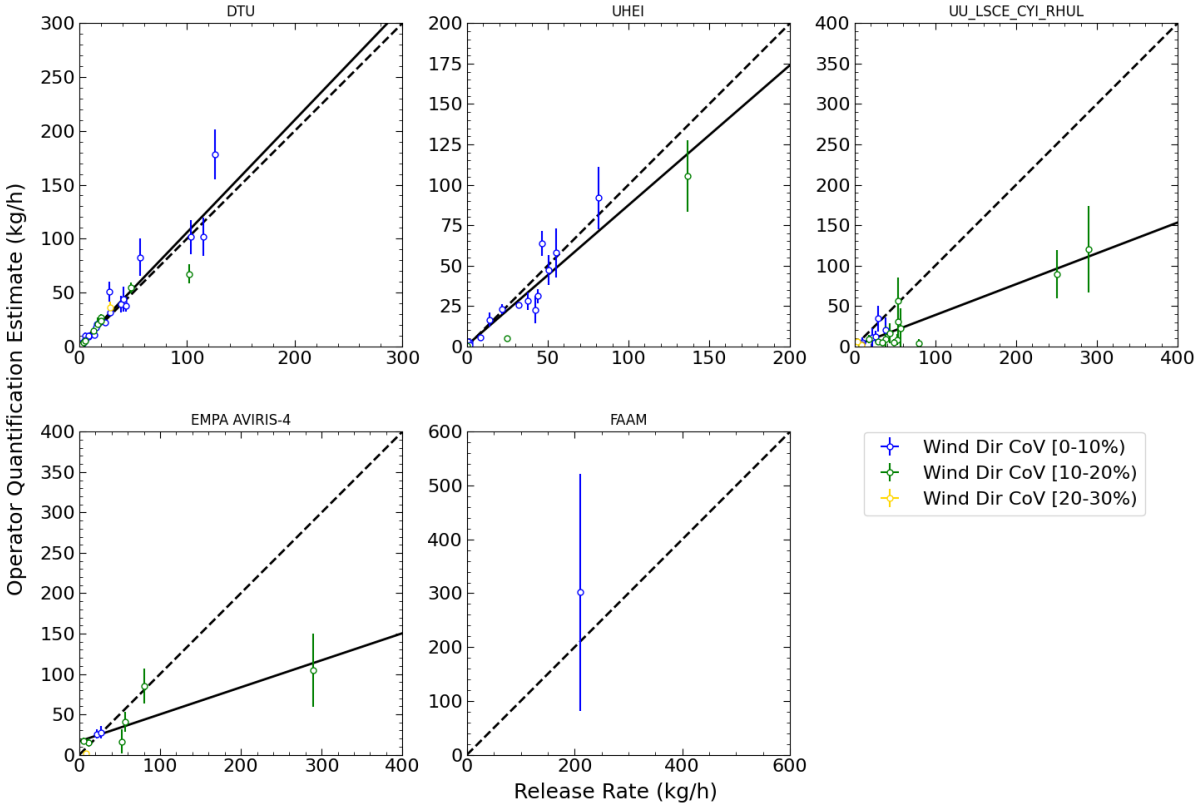



**Figure S31.** Parity plots with wind direction coefficient of variation (CoV).
The average wind direction CoVs are binned into low [0-10%), medium [10-20%), and high [20-30%) wind direction CoV ranges.

In addition to providing context about each of the quantification estimates submitted by a participant, this wind analysis allowed us to investigate the impact of varying wind conditions on quantification performance. For example, to view the impact of average wind speed on quantification ability, a participant's estimates were categorized into different average wind speed bins, and the best fit line was recalculated using only those data points, yielding a slope and $R^2$ value for each bin. These calculations were performed for each participant and average wind speed, wind speed CoV, and wind direction CoV bin. Table S25 summarizes these results. The scale and sometimes direction of improvement varies by participant. Additionally, many of the participants had only a few data points in a bin; although slope and $R^2$ values were calculated for any bin with >1 datapoint, it is difficult to draw any conclusion (see Table S26 for the number of data points in each bin for each participant). The impact of wind conditions on quantification performance is more evident and robust when combining the release rate estimates across all participants. In general, quantification performance improves as average wind speed increases, wind speed CoV decreases, and wind direction CoV decrease. Improved performance is indicated by best fit line slopes closer to 1.00 and $R^2$ values closer to 1.

**Table S25. Slope ($R^2$) values of the linear model fit on releases across technology types and wind analysis bins. Values are provided for bins that had more than one quantification estimate occurring under those wind conditions. FAAM only submitted one estimate, so a linear trend could not be fit to the data.**

| | Wind Speed Average Bins | | | Wind Speed CoV Bins | | Wind Direction CoV Bins | | |
|---|---|---|---|---|---|---|---|---|
| **Solution** | **[0-2) m/s** | **[2-4) m/s** | **[4-6) m/s** | **[0-25%)** | **[25-50%)** | **[0-10%)** | **[10-20%)** | **[20-30%)** |
| *DTU* | 0.85 (0.91) | 1.12 (0.94) | 0.75 (0.70) | 0.96 (1.00) | 1.06 (0.87) | 1.13 (0.93) | 0.68 (0.89) | - |
| *UHEI* | - | 0.81 (0.90) | 1.16 (0.96) | 1.10 (0.96) | 0.81 (0.89) | 1.03 (0.89) | 0.81 (0.98) | - |
| *UU/LSCE/CYI/RHUL* | 0.33 (0.80) | 0.42 (0.92) | - | 0.55 (0.49) | 0.38 (0.88) | 0.67 (0.72) | 0.39 (0.87) | -0.82 (1.00) |
| *Empa/UZH* | 0.13 (0.15) | 0.30 (0.76) | - | 0.33 (0.74) | - | 0.41 (1.00) | 0.32 (0.72) | - |
| *FAAM* | - | - | - | - | - | - | - | - |

**Table S26. Number of data points in the bins of average wind speed, wind speed CoV, and wind direction CoV used in analysis.**

| | Wind Speed Average Bins | | | Wind Speed CoV Bins | | | | Wind Direction CoV Bins | | |
|---|---|---|---|---|---|---|---|---|---|---|
| **Solution** | **[0-2) m/s** | **[2-4) m/s** | **[4-6) m/s** | **[0-25%)** | **[25-50%)** | **[50-75%)** | **[75-100%)** | **[0-10%)** | **[10-20%)** | **[20-30%)** |
| *DTU* | 3 | 25 | 9 | 9 | 25 | 1 | 2 | 27 | 9 | 1 |
| *UHEI* | 0 | 15 | 3 | 5 | 13 | 0 | 0 | 15 | 3 | 0 |
| *UU/LSCE/CYI/RHUL* | 21 | 11 | 0 | 3 | 29 | 0 | 0 | 10 | 20 | 2 |
| *Empa/UZH* | 3 | 6 | 0 | 0 | 9 | 0 | 0 | 2 | 6 | 1 |
| *FAAM* | 0 | 1 | 0 | 1 | 0 | 0 | 0 | 1 | 0 | 0 |

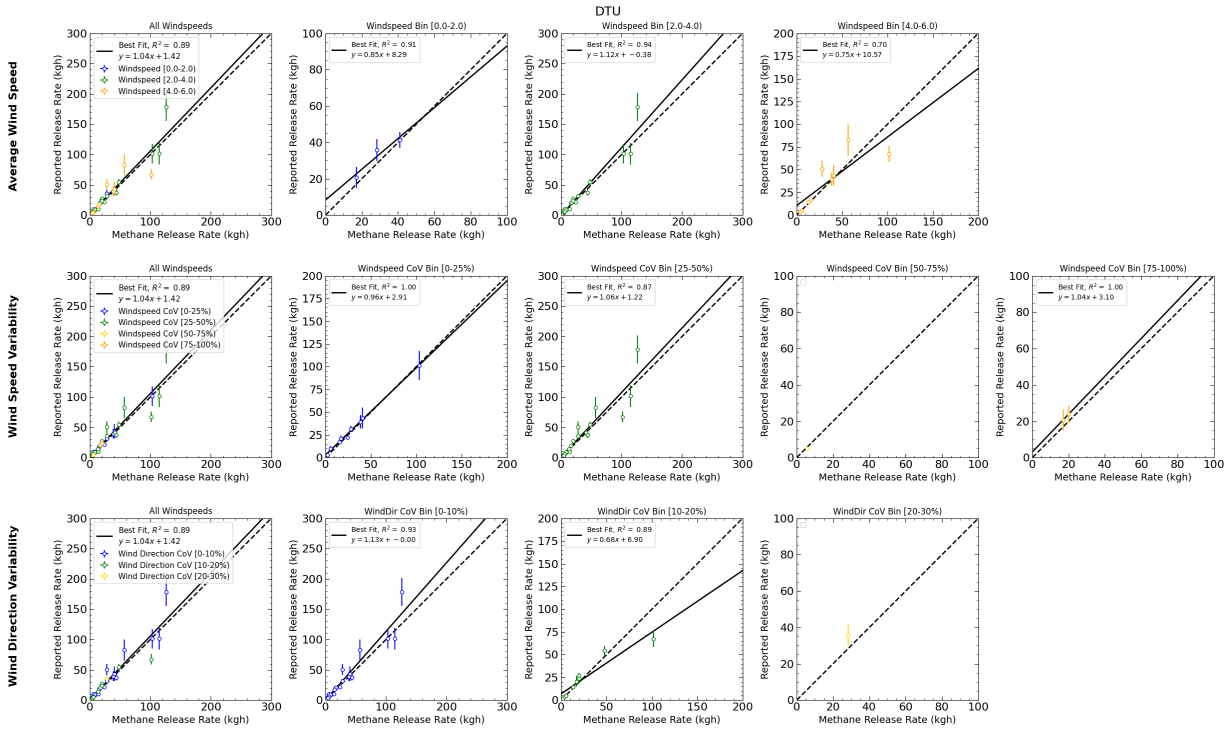



**Figure S32.** DTU quantification data by wind condition bin.

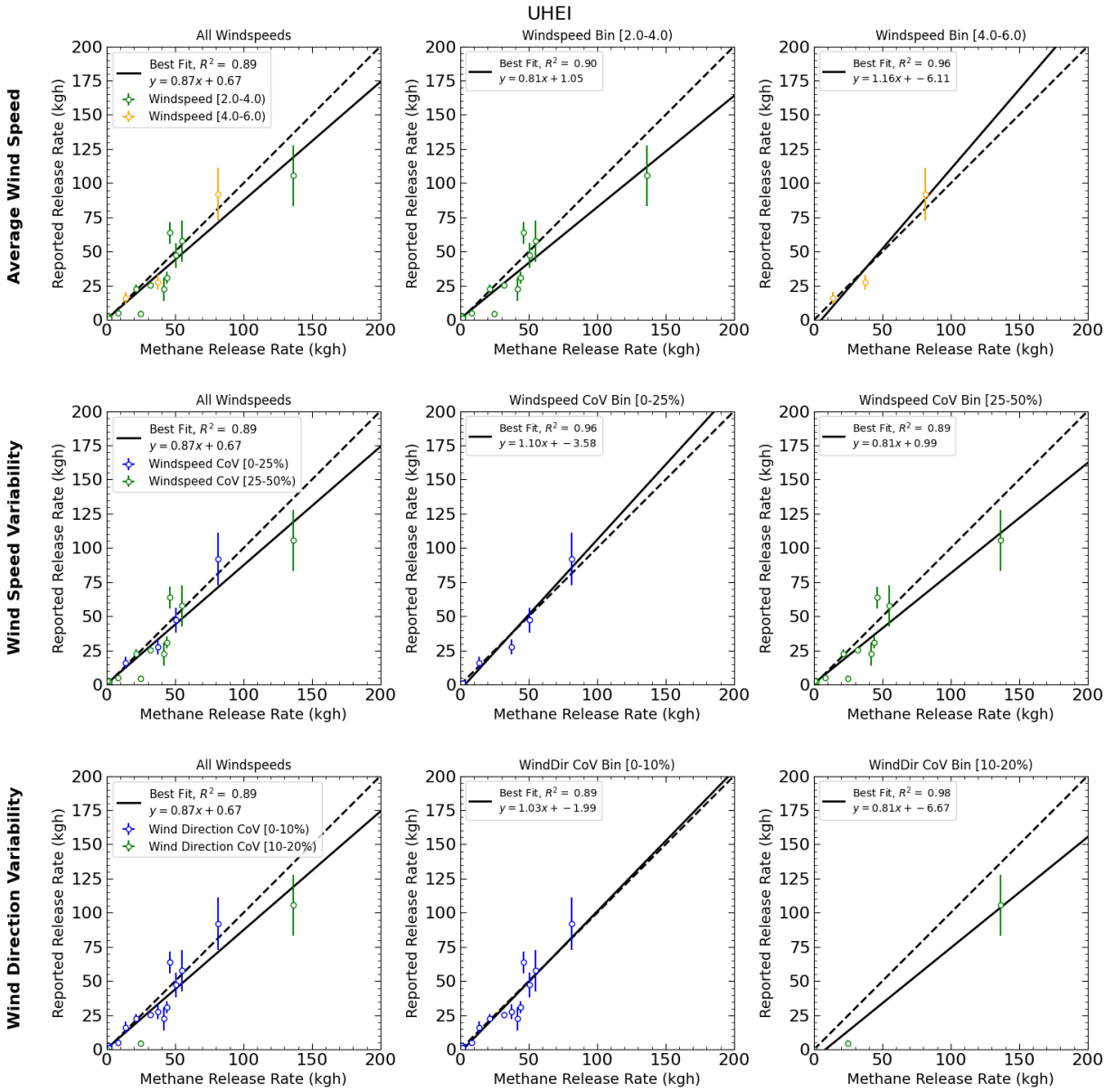



**Figure S33.** UHEI quantification data by wind condition bin.

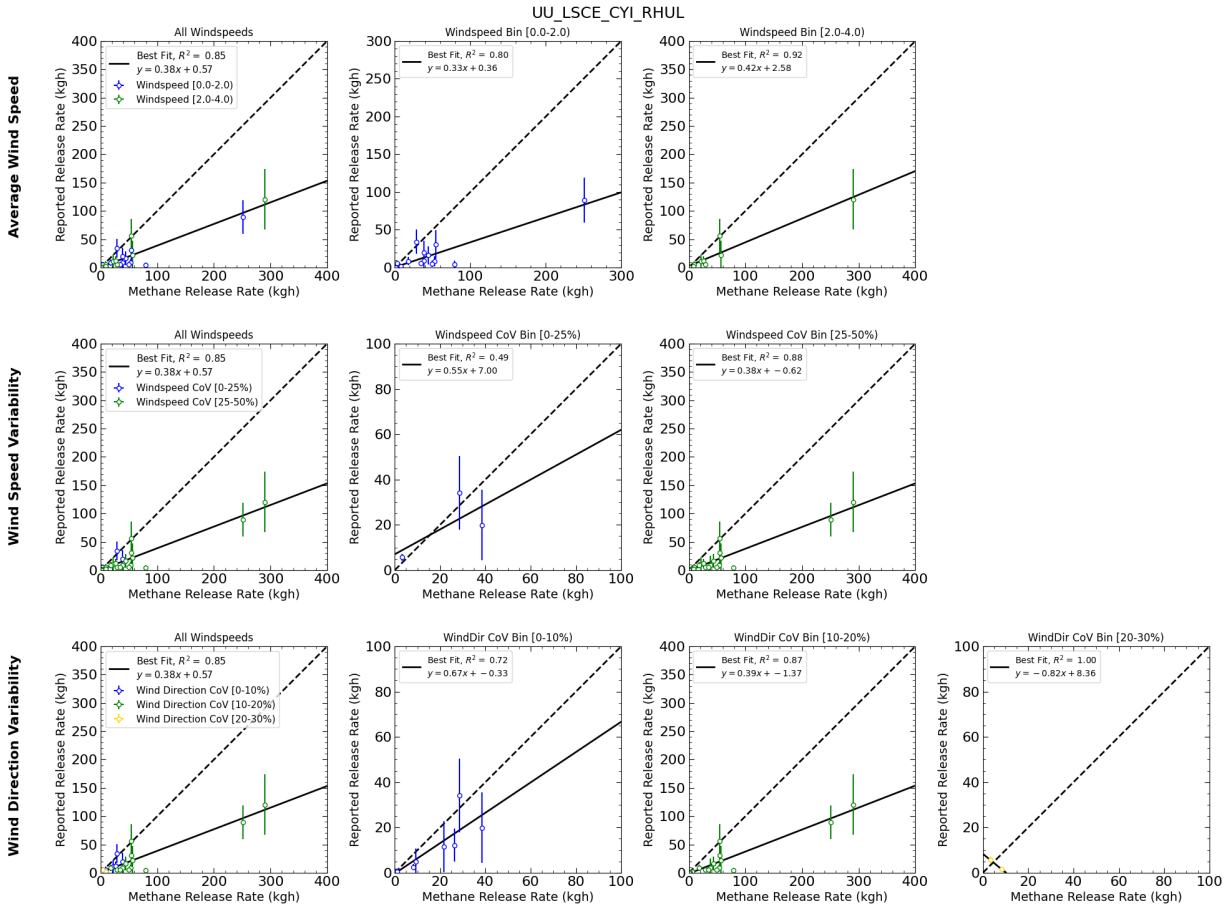



**Figure S34.** UU/LSCE/CYI/RHUL quantification data by wind condition bin.

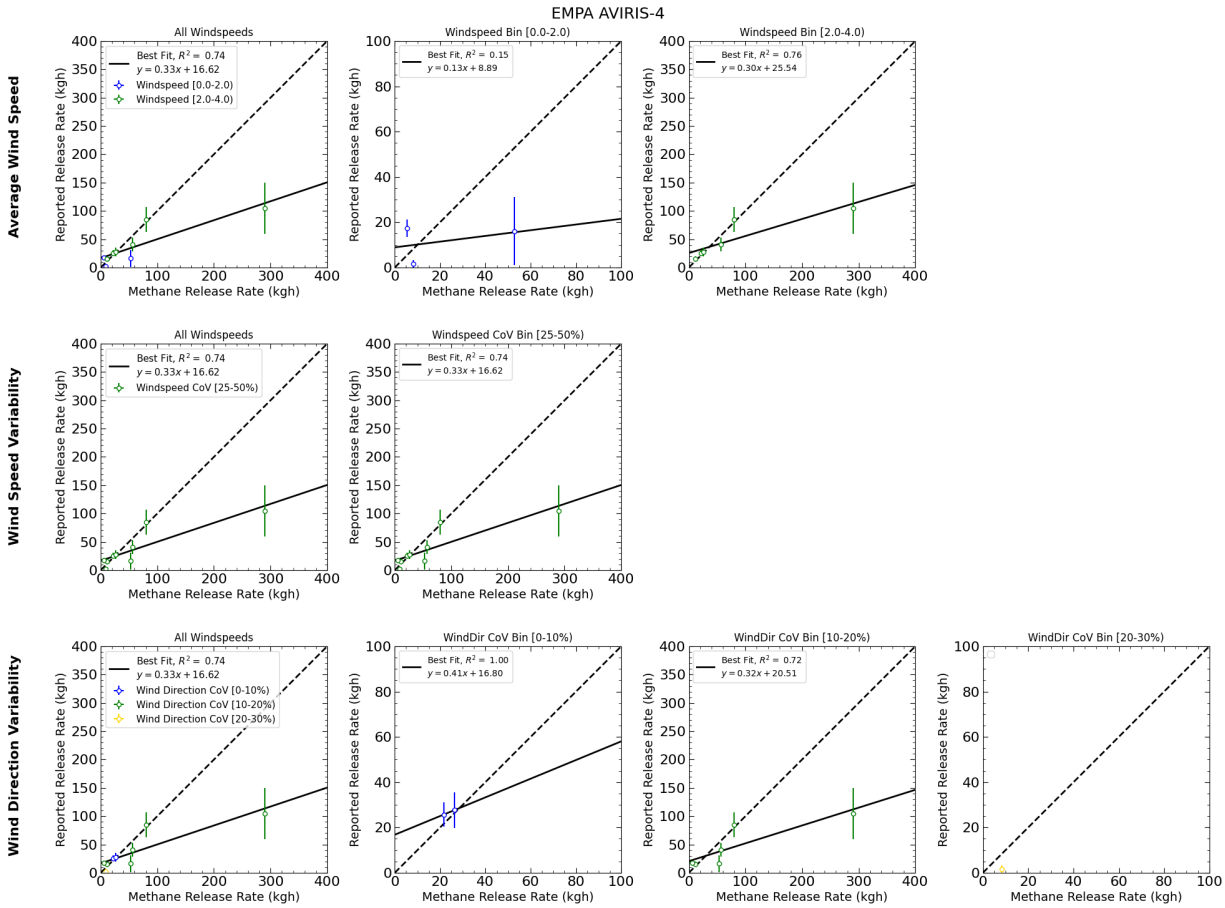



**Figure S35.** Empa/UZH quantification data by wind condition bin.

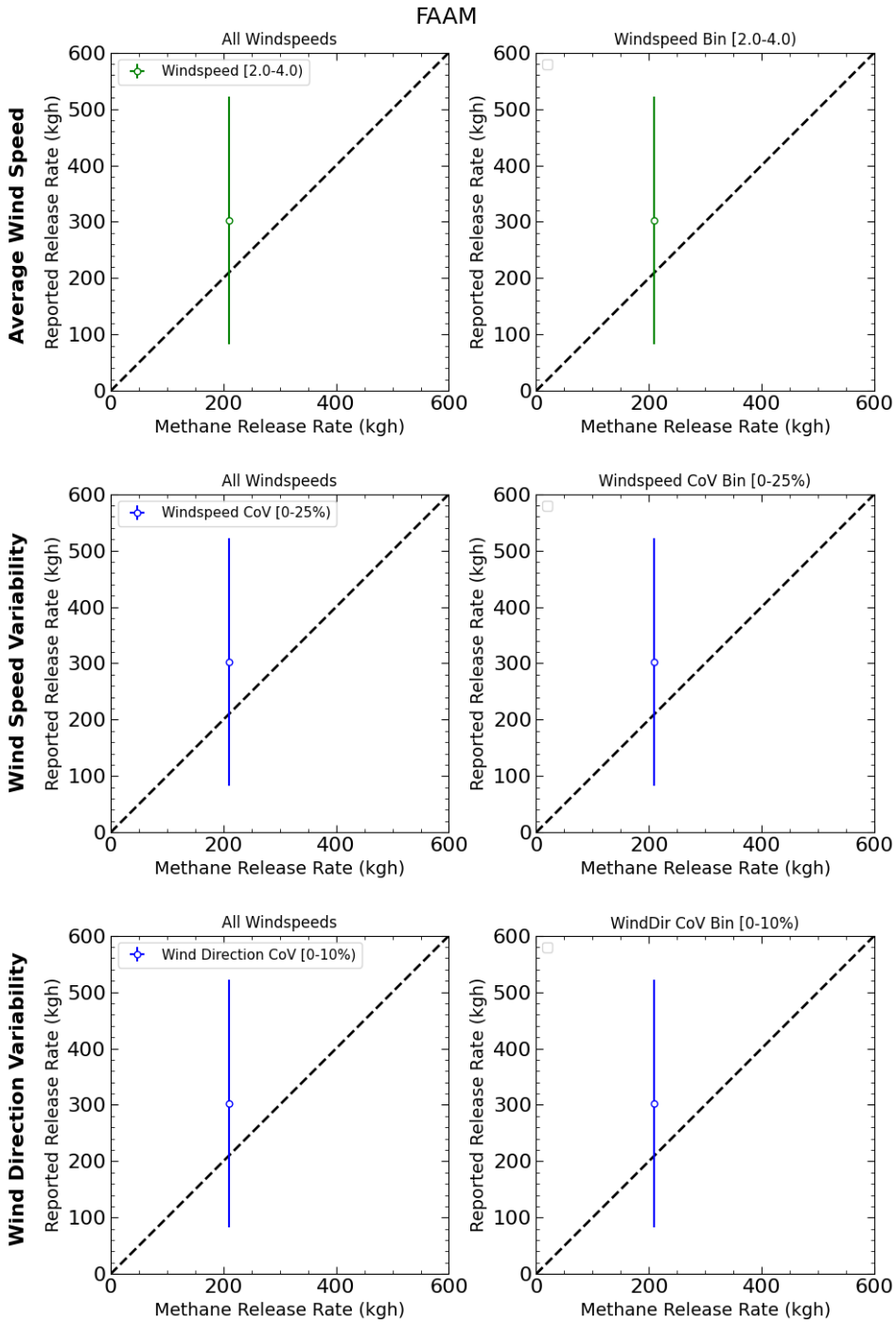



**Figure S36.** FAAM quantification data by wind condition bin.

**References**


Bauguitte, S.: SO2 Instrument Description, Zenodo, https://doi.org/10.5281/zenodo.7391495, 2022.

Bauguitte, S.: 2B Ozone Instrument description, Zenodo, https://doi.org/10.5281/zenodo.7503437, 2023.

CERC: ADMS model, https://www.cerc.co.uk/environmental-software/ADMS-model.html (last access: 21 January 2026), 2026.

Delre, A., Mønster, J., Samuelsson, J., Fredenslund, A. M., and Scheutz, C.: Emission quantification using the tracer gas dispersion method: The influence of instrument, tracer gas species and source simulation, Sci. Total Environ., 634, 59–66, https://doi.org/10.1016/j.scitotenv.2018.03.289, 2018.

Drummond, J. W., Volz, A., and Ehhalt, D. H.: An optimized chemiluminescence detector for tropospheric NO measurements, J. Atmos. Chem., 2, 287–306, https://doi.org/10.1007/BF00051078, 1985.

DTU Sustain: About the department, https://sustain.dtu.dk/en/om-os (last access: 29 January 2025), 2025.

Empa: Air Pollution / Environmental Technology – Remote Sensing, https://www.empa.ch/web/s503/remote-sensing (last access: 29 January 2025), 2025.

FAAM: About FAAM, https://www.faam.ac.uk/what-is-faam/ (last access: 29 January 2025), 2025.

Foote, M. D., Dennison, P. E., Thorpe, A. K., Thompson, D. R., Jongaramrungruang, S., Frankenberg, C., and Joshi, S. C.: Fast and Accurate Retrieval of Methane Concentration From Imaging Spectrometer Data Using Sparsity Prior, IEEE Trans. Geosci. Remote Sens., 58, 6480–6492, https://doi.org/10.1109/TGRS.2020.2976888, 2020.

Fredenslund, A., Gudmundsson, E., Falk, J. M., and Scheutz, C.: The Danish national effort to minimise methane emissions from biogas plants, Waste Manag., 157, 321–329, https://doi.org/10.1016/j.wasman.2022.12.035, 2023.

Fredenslund, A. M., Rees-White, T. C., Beaven, R. P., Delre, A., Finlayson, A., Helmore, J., Allen, G., and Scheutz, C.: Validation and error assessment of the mobile tracer gas dispersion method for measurement of fugitive emissions from area sources, Waste Manag., 83, 68–78, https://doi.org/10.1016/j.wasman.2018.10.036, 2019.

Heidelberg University, Institute of Environmental Physics: Institute of Environmental Physics, https://www.iup.uni-heidelberg.de/en (last access: 29 January 2025), 2025.

Kissas, K., Ibrom, A., Kjeldsen, P., and Scheutz, C.: Methane emission dynamics from a Danish landfill: The effect of changes in barometric pressure, Waste Manag., 138, 234–242, https://doi.org/10.1016/j.wasman.2021.11.043, 2022.

Korbeń, P., Jagoda, P., Maazallahi, H., Kammerer, J., Nęcki, J. M., Wietzel, J. B., Bartyzel, J., Radovici, A., Zavala-Araiza, D., Röckmann, T., and Schmidt, M.: Quantification of methane emission rate from oil and gas wells in Romania using ground-based measurement techniques, Elem. Sci. Anthr., 10, 00070, https://doi.org/10.1525/elementa.2022.00070, 2022.

Kuhlmann, G., Koene, E., Meier, S., Santaren, D., Broquet, G., Chevallier, F., Hakkarainen, J., Nurmela, J., Amorós, L., Tamminen, J., and Brunner, D.: The *ddeq* Python library for point source quantification from remote sensing images (version 1.0), Geosci. Model Dev., 17, 4773–4789, https://doi.org/10.5194/gmd-17-4773-2024, 2024.

LSCE: The laboratory, https://www.lsce.ipsl.fr/en/the-laboratory/ (last access: 30 January 2025), 2025.

McManemin, A., Juéry, C., Blandin, V., France, J. L., Burdeau, P., and Brandt, A. R.: Controlled release testing of commercially available methane emission measurement technologies at the TADI facility, Atmos. Meas. Tech., 19, 923–934, https://doi.org/10.5194/amt-19-923-2026, 2026.

Mønster, J. G., Samuelsson, J., Kjeldsen, P., Rella, C. W., and Scheutz, C.: Quantifying methane emission from fugitive sources by combining tracer release and downwind measurements – A sensitivity analysis based on multiple field surveys, Waste Manag., 34, 1416–1428, https://doi.org/10.1016/j.wasman.2014.03.025, 2014.

Morales, R., Ravelid, J., Vinkovic, K., Korbeń, P., Tuzson, B., Emmenegger, L., Chen, H., Schmidt, M., Humbel, S., and Brunner, D.: Controlled-release experiment to investigate uncertainties in UAV-based emission quantification for methane point sources, Atmos. Meas. Tech., 15, 2177–2198, https://doi.org/10.5194/amt-15-2177-2022, 2022.

O'Shea, S. J., Bauguitte, S. J.-B., Gallagher, M. W., Lowry, D., and Percival, C. J.: Development of a cavity-enhanced absorption spectrometer for airborne measurements of CH4 and CO2, Atmos. Meas. Tech., 6, 1095–1109, https://doi.org/10.5194/amt-6-1095-2013, 2013.

Pollack, I. B., Lerner, B. M., and Ryerson, T. B.: Evaluation of ultraviolet light-emitting diodes for detection of atmospheric NO2 by photolysis - chemiluminescence, J. Atmos. Chem., 65, 111–125, https://doi.org/10.1007/s10874-011-9184-3, 2010.

Price, H. C.: Temperature and humidity measurements on the FAAM aircraft, Zenodo, https://doi.org/10.5281/zenodo.5846962, 2022.

Ridley, B. A. and Grahek, F. E.: A Small, Low Flow, High Sensitivity Reaction Vessel for NO Chemiluminescence Detectors, Journal of Atmospheric and Oceanic Technology, 7, 307–311, https://doi.org/10.1175/1520-0426(1990)007%253C0307:ASLFHS%253E2.0.CO;2, 1990.

Rosenberg, P. D., Dean, A. R., Williams, P. I., Dorsey, J. R., Minikin, A., Pickering, M. A., and Petzold, A.: Particle sizing calibration with refractive index correction for light scattering optical particle counters and impacts upon PCASP and CDP data collected during the Fennec campaign, Atmos. Meas. Tech., 5, 1147–1163, https://doi.org/10.5194/amt-5-1147-2012, 2012.

Royal Holloway University of London: Department of Earth Sciences, https://pure.royalholloway.ac.uk/en/organisations/department-of-earth-sciences (last access: 29 January 2025), 2025.

Royal Holloway University of London: Greenhouse Gas Research Group – Facilities, https://ggrg.rhul.ac.uk/facilities/ (last access: 21 January 2026), 2026.

Ryder, C. L., Highwood, E. J., Rosenberg, P. D., Trembath, J., Brooke, J. K., Bart, M., Dean, A., Crosier, J., Dorsey, J., Brindley, H., Banks, J., Marsham, J. H., McQuaid, J. B., Sodemann, H., and Washington, R.: Optical properties of Saharan dust aerosol and contribution from the coarse mode as measured during the Fennec 2011 aircraft campaign, Atmos. Chem. Phys., 13, 303–325, https://doi.org/10.5194/acp-13-303-2013, 2013.

Shaw, J. T., Allen, G., Barker, P., Pitt, J. R., Pasternak, D., Bauguitte, S. J.-B., Lee, J., Bower, K. N., Daly, M. C., Lunt, M. F., Ganesan, A. L., Vaughan, A. R., Chibesakunda, F., Lambakasa, M., Fisher, R. E., France, J. L., Lowry, D., Palmer, P. I., Metzger, S., Parker, R. J., Gedney, N., Bateson, P., Cain, M., Lorente, A., Borsdorff, T., and Nisbet, E. G.: Large Methane Emission Fluxes Observed From Tropical Wetlands in Zambia, Glob. Biogeochem. Cycles, 36, e2021GB007261, https://doi.org/10.1029/2021GB007261, 2022.

Swiss Flight Services: Company, https://www.sfsaviation.ch/Company (last access: 29 January 2025), 2025.

The Cyprus Institute: Overview and mission, https://www.cyi.ac.cy/index.php/cyi/about-the-institute/institute-overview.html (last access: 29 January 2025), 2025.

TotalEnergies: TADI: A test center with international reach in Lacq, https://cstjf-pau.totalenergies.fr/en/our-expertise/leveraging-digital-innovation/tadi-test-center-international-reach-lacq (last access: 29 January 2025), 2025a.

TotalEnergies: Methane Emissions Reduction: TotalEnergies and Colorado State University collaborate to establish a protocol of qualification for methane measurement technologies, https://totalenergies.com/media/news/press-releases/methane-emissions-reduction-totalenergies-and-colorado-state-university (last access: 29 January 2025), 2025b.

University of York, Wolfson Atmospheric Chemistry Laboratories: Services, https://www.york.ac.uk/chemistry/research/wacl/services/#tab-1 (last access: 21 January 2026), 2026.

University of Zurich: Remote Sensing, Department of Geography, https://www.geo.uzh.ch/en/units/rs.html (last access: 29 January 2025), 2025.

Utrecht University: About us – Organisation, https://www.uu.nl/en/organisation/about-us (last access: 29 January 2025), 2025.

van Heerwaarden, C. C., van Stratum, B. J. H., Heus, T., Gibbs, J. A., Fedorovich, E., and Mellado, J. P.: MicroHH 1.0: a computational fluid dynamics code for direct numerical simulation and large-eddy simulation of atmospheric boundary layer flows, Geosci. Model Dev., 10, 3145–3165, https://doi.org/10.5194/gmd-10-3145-2017, 2017.

Wietzel, J. B., Korbeń, P., Hoheisel, A., and Schmidt, M.: Best practices and uncertainties in $CH_4$ emission quantification: employing mobile measurements and Gaussian plume modelling at a biogas plant, Atmos. Meas. Tech., 18, 4631–4645, https://doi.org/10.5194/amt-18-4631-2025, 2025.

Zimmerle, D., Levin, E., Emerson, E., Juéry, C., Marcarian, X., and Blandin, V.: Controlled Test Protocol: Emission Detection and Quantification Protocol (version 1.2), 2025. https://metec.colostate.edu/wp-content/uploads/sites/37/2025/04/Combined-Monitoring-Protocol-V1.2_Final.pdf.